INTERPRETATION SCHEME FORMULATION FOR THE DPM SERIES OF EM PROSPECTING TOOLS USING A SIMPLE MODEL

A Thesis

Submitted to the

Faculty of Graduate Studies and Research

The University of Manitoba

In Partial Fulfillment

of the Requirements for the Degree of

Master of Science

by

Dean Allen Provins

March, 1971

TABLE OF CONTENTS

LIST OF TABLES

LIST OF FIGURES

ABSTRACT

The DPM series of geophysical prospecting instruments are receivers designed to examine some or all of the characteristics of the time-varying magnetic field ellipse generated by a fixed source which is either a long grounded wire or large rectangular loop. The DPM-1 receiver measures the dip-angle of the field ellipse, while the DPM-2 receiver measures the values of the major and minor axes of the ellipse as well as the dip angle. Measurements are made in a vertical plane normally at right angles to the source.

As a prelude to planned lab scale model studies for the DPM series, a study using a linear current concentration to represent a responding body was instituted using the University's IBM 360/65 computer. The fit of a computed anomaly to DPM-1 field data and the similarity of computed responses to DPM-2 field data suggests that this model, while simple, is not an unreasonable first approximation.

The characteristics of responses over conductors of different quality were noted with a view to setting up an interpretation scheme. It was observed that the differences in position for the half maximum slope positions about the point of maximum slope in the dip-angle profile appeared to increase linearly with depth for shallow depths. It was

also noted that the differences in position of the maximum and minimum slopes in the dip-angle profile seemed to vary with depth and conductor quality, which suggested that plots of these versus half maximum slope differences might be useful. While conductor quality was not found to be well-defined, this approach would be useful for making depth estimates to conductors from DPM-1 data. It was found that plots of in-phase and quadrature maxima normalized to the primary field in-phase component magnitude was the best method of estimating both depth and quality.

The position of the point of inflexion in the dip-angle profile was observed to located approximately over the conductor axis for shallow depths. The maximum depth for which this was the case decreased as the primary field dip angle increased, but the conductor axis was always located between the point of maximum slope and the point of half maximum slope furthest from the source.

ACKNOWLEDGEMENTS

The writer wishes to express his thanks to Dr. C. D. Anderson of the Department of Earth Sciences for his suggestions and assistance during the course of the study. Thanks are due also to Central Geophysics Limited of Winnipeg Manitoba for the opportunity to use a prototype DPM-2 field instrument.

During the course of his study, the author was supported by a University of Manitoba Graduate Fellowship from the Department of Earth Sciences, University of Manitoba.

CHAPTER I

INTRODUCTION

DPM-2 is a receiver system designed to measure the properties of the time-varying magnetic field ellipse produced by a long grounded wire or large loop source. It will respond to bodies at depths which are ordinarily considered to be too great to produce a measureable response in many systems (for example, Horizontal Loop). Examination of the characteristics of the field ellipse is made by rotating a pair of orthogonal coils until they are aligned with the axes of the ellipse. While an easy to use prospecting tool, it has taken some time to develop field instruments that are uncomplicated and fast to use. In the early 1900's, the idea of examining the magnetic field ellipse was first considered.

Sundberg (1931) discusses early galvanic methods and notes that occasional surveys were comprised of the determination of the azimuth and dip of the field ellipse. For detailed work, a complete determination of the field ellipse was made by either measuring the amplitudes of the axes of the ellipse or by measurement of the amplitude and phase of any two component vectors. This manner of surveying was limited for technical reasons. Likely the difficulties

experienced are typified by those reported for the Bieler-Watson method (Parasnis, 1966), a prospecting tool used in Australia in the 1930's.

The Bieler-Watson method was designed to measure the quadrature to in-phase ratio of the polarization ellipse using two mutually orthogonal coils. One coil was tuned to the primary frequency and the other, having multiple taps, was used to obtain a null between the two induced signals, by varying the number of turns in the coil. The difficulty with the system was that of deteriming the ellipse orientation, a difficulty removed by modern electronic circuits. Because the search for the ellipse orientation delayed the field work, operation was modified to measure the component of the horizontal field in phase with the total vertical field.

In more recent times, other methods have been developed which rely upon the orientation of the field ellipse.

In the late 1950's, the Afmag method was developed and is still in limited use. It is an azimuth-dip angle method that examines the ellipse orientation in reconnaissance surveys. An inexpensive method, it is a one-man, receiver-only system that relies on a naturally produced low frequency, sferic energy source. It is this source which has proven to be the major drawback in its acceptance because of its unreliability. It has both diurnal and annual fluctuations in intensity and azimuth as well as a latitude variation, weakening towards the poles.

At about the same time, both the British and United States governments set up very low frequency (VLF) radio stations to communicate with their respective defense forces. These stations proved to be a useful source for the VLF method.

The stations transmit unmodulated carrier waves, either continuously or with Morse code, at frequencies from 15-25 kHz. The horizontally oriented magnetic vector is a component of the plane wave (at great distances) radiated by the station transmitter. Interaction of this electromagnetic wave with a conducting responder results in the generation of an anomalous secondary field. The net result is an elliptically polarized, time-varying magnetic vector which varies in spatial orientation over the responder.

Studies in Sweden by the Swedish Geological Survey, involved both measuring the horizontal component of the field, and examining the orientation of the ellipse. The latter was accomplished by varying the orientation of a receiver coil until a tone minimum was heard in a speaker. Broadening of the ellipse, due to an increased quadrature component, tends to broaden the region in which an apparent tone minimum is heard, thus making the method inaccurate.

Commercial receivers in North America sharpen the tone minimum by using a crossed-coil receiver and compensating for the quadrature component of the field ellipse. In the case of the Ronka EM-16, the tangent of the dip angle and the ellipticity are the recorded measurements. To a good

approximation, these are the in-phase and out-phase components of the vertical field. While a useful method, it has several limitations. Because of the high frequencies employed, it is subject to picking up unwanted responses. Swampy areas, which have a low conductivity, become responders at VLF operating frequencies. In addition, a VLF survey, like most other geophysical surveys, must be run at or near right angles to the geologic strike, for good anomaly resolution, and interpretation purposes. This requires that a transmitting station be in-line, or nearly in-line with the local strike. If the available stations are not suitably positioned, or a suitable station is not on the air or is too weak to receive, a survey cannot be run. Finally, accurate readings may be difficult to take in regions of high quadrature, because compensation for this component is insufficient to sharpen the tone minimum for the accurate orientation of the instrument.

However, the successes of recent developments have indicated the usefulness of the orientation of the field ellipse, and with the advent of reliable, and miniaturized circuitry as well as with the use of reliable sources, the DPM series of instruments have been developed. The DPM-1 receiver is a tilt angle measuring device and the DPM-2 is a receiver which also examines the elliptically of the field. Both instruments operate at low frequencies, and use strong fixed sources.

CHAPTER II

PROSPECTING METHOD

Typical surveys to date have used a long grounded wire from one to five miles in length, depending on the size of the prospect to be surveyed. Generally, #25 AWG enamelled copper wire serves as a source cable, and this is earthed via copper-coated electrodes about three feet long. Often, one electrode at each end, driven into moist soil or overburden, will suffice, although a brine solution and a multi-electrode array (3 or 4 electrodes) may be necessary in special cases.

The source cable acts as an antenna driven by a solid state transmitter operating at fixed frequencies, typically 500 Hz, with a lower frequency near 120 Hz available and a higher frequency near 2000 Hz being considered. The power for the transmitter is derived from a wet cell, usually a car battery, which lasts from one to two days under normal operating conditions before requiring a recharge. The load resistance required by the transmitter is not critical, and may range from 700 to 1200 ohms, values which are easily achieved by proper positioning of the electrodes.

Receivers are orthogonal coil assemblies having built-in clinometers for dip angle measurements. These are

coupled to battery-powered chest pack consoles containing the phase shifting circuits and read-out devices necessary for an accurate determination of the ellipse orientation. Other circuits and meters allow measurements to be made of the magnitudes of the major and minor axes of the ellipse, aligned with the two coils.

Typical surveys are run along lines perpendicular to strike, with the source cable running parallel to strike. Stations are generally read at 100 ft intervals, and the lines are usually separated by 400 ft. For greater detail, 50 ft spacing between stations is used, and additional lines may be run at 100-200 ft intervals.

Because of the wide electrode spacing as compared to typical ore-body lengths of 600-1000 ft (Bosschart, 1964), unless a body is near one electrode, little conductive response can be expected. What little current is carried by the responder will likely tend only to enhance the anomaly, making it more easily discernible, and possibly improve its apparent quality (Parasnis, 1966).

CHAPTER III

THE SOURCE FIELD

An expression for the time-varying magnetic field of an infinitely long cable must describe its rate of fall-off in strength, its polarization, and orientation. Bursian (1934) obtained such an expression, noting that the field's elliptical polarization and orientation over a homogeneous halfspace was dependent upon its distance from the cable, and the electrical properties of the halfspace. More recently, Ryu *et al.* (1970) have obtained detailed expressions for the electric and magnetic fields over an n-layered halfspace for a loop source.

Bezvoda (1970) expresses the normal field of the infinitely long cable at the boundary of the halfspace simply as

$$\vec{H}(y) = \frac{2I\vec{h}(\xi)}{cy} \qquad \ldots 1$$

where,

I = current in the cable

c = speed of light

y = perpendicular distance from the cable

h = a complex function depending on the transformed co-ordinate ξ, and which represents a departure from the normal field of an infinitely long cable

due to the halfspace interface.

The dimensionless number ξ, is expressed as

$$\xi = y(2\pi\mu f\sigma)^{\frac{1}{2}} \qquad \ldots 2$$

where,

μ = permeability, generally the free space value (henries/m)

σ = conductivity of the halfspace (mho/m)

f = frequency (Hz)

For a frequency of 660 Hz, and several values of δ, the vector $h(\xi)$ is plotted in Fig. 1. The resulting field is elliptical, with 'A' and 'B' representing the major and minor axes of the ellipse. The dashed line in the figure is the minor axis 'B' multiplied by a factor of three.

From Fig. 1 and equation 2, it can be noted that the rate of fall-off in both dip angle and field strength is governed by the average ground conductivity. This rate of decay may be related to the skin depth 'δ', given by

$$\delta = \frac{\sqrt{2}}{\sqrt{\sigma\mu\omega}} \qquad \ldots 3$$

where,

ω = frequency in radians per second.

Consequently, ξ and δ are related by

$$\xi = \frac{\sqrt{2}\cdot y}{\delta} \qquad \ldots 4$$

Fig. 1. The vector $\vec{h}(\xi)$ for an infinite straight cable as a function of distance for the resistivities 33, 100, 1200 ohm-meters (corresponding to conductivities of 0.03, 0.01, and 0.0008 mho/meter) at 660 Hz. The dashed line is the minor axis multiplied by 3. (after Bezvoda, 1970)

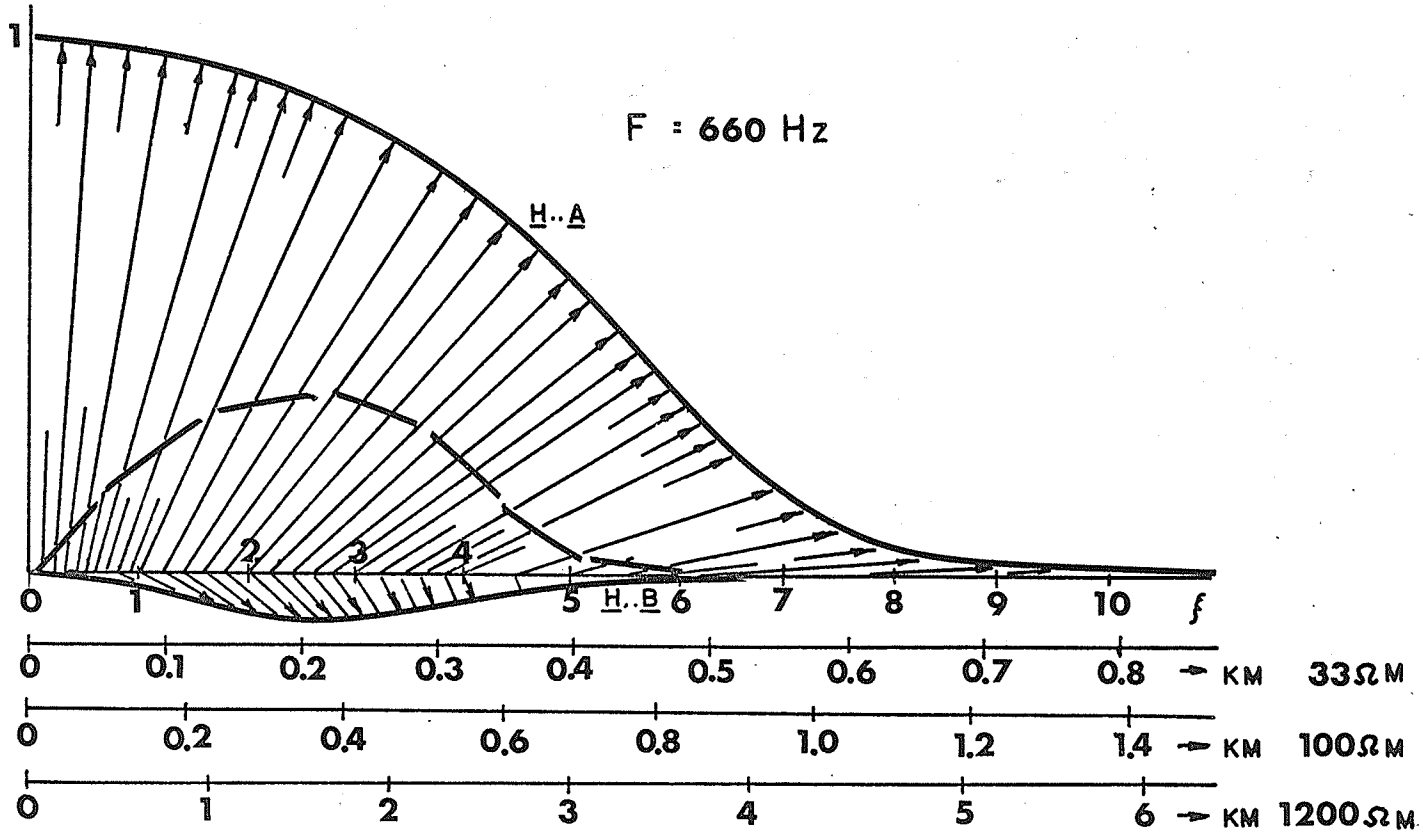
1
F = 660 Hz
H..A
2
3
4
0
1
5
H..B
6
7
8
9
10
f
0
0.1
0.2
0.3
0.4
0.5
0.6
0.7
0.8
KM
33Ω M
0
0.2
0.4
0.6
0.8
1.0
1.2
1.4
KM
100Ω M
0
1
2
3
4
5
6
KM
1200Ω M

It follows that the greater the skin depth, the lesser the rate of fall-off in dip angle and field strength.

From Fig. 1, it may also be seen that the ellipticity of the field varies with the displacement from the wire. Near the source, and at large distances from it, the field is almost linearly polarized, while at dip angles near 45^{o}, the ellipticity reaches approximately 10%. This value is not so large as to prevent accurate measurements of the field orientation from being made. However, the addition of anomalous secondary fields varying in strength and phase with the primary field may occasionally, although rarely, prevent measurements from being made. This occurs in regions of conductive overburden where eddy currents are strong, or over poor but shallow responders which as a result, also have out-of-phase eddy currents. It also occurs during periods of exceptional sferic energy discharges having frequency components at the operating frequency when the receiver is near poor conductors.

The field of a large loop source has been considered more recently, specifically with regard to inductive sounding. The results obtained by Ryu *et al.* (1970) are indicative of the value of ellipticity and tilt angle readings when they show that measurements of these two parameters allow good resolution of subsurface layering. It is to be expected that they would be as useful in the location of ore-bodies.

Field Curves

Figure 2 shows the DPM-1 field curve over a strong conducting body. In Fig. 3, DPM-2 measurements are shown. In-phase and quadrature maxima appear to sit on opposite sides of the conductor axis which is generally picked as the point of maximum inflexion in the dip angle profile. Figure 4 demonstrates the occasional effects of an unusually strong sferic background. In Fig. 4a may be seen the result of high quadrature components which make the elliptical field degenerate towards a circularly polarized field. Consequently, unless the instrument has exceedingly high resolution of vector magnitude, a measurement of the ellipse orientation may not be made. The effects of a much weaker sferic background are not discernible in Fig. 4b, where measurements over the same body and at the same stations were made on a different day.

Fig. 2. DPM-1 field curve over a strong conductor (after Anderson and Sutherland, 1970).

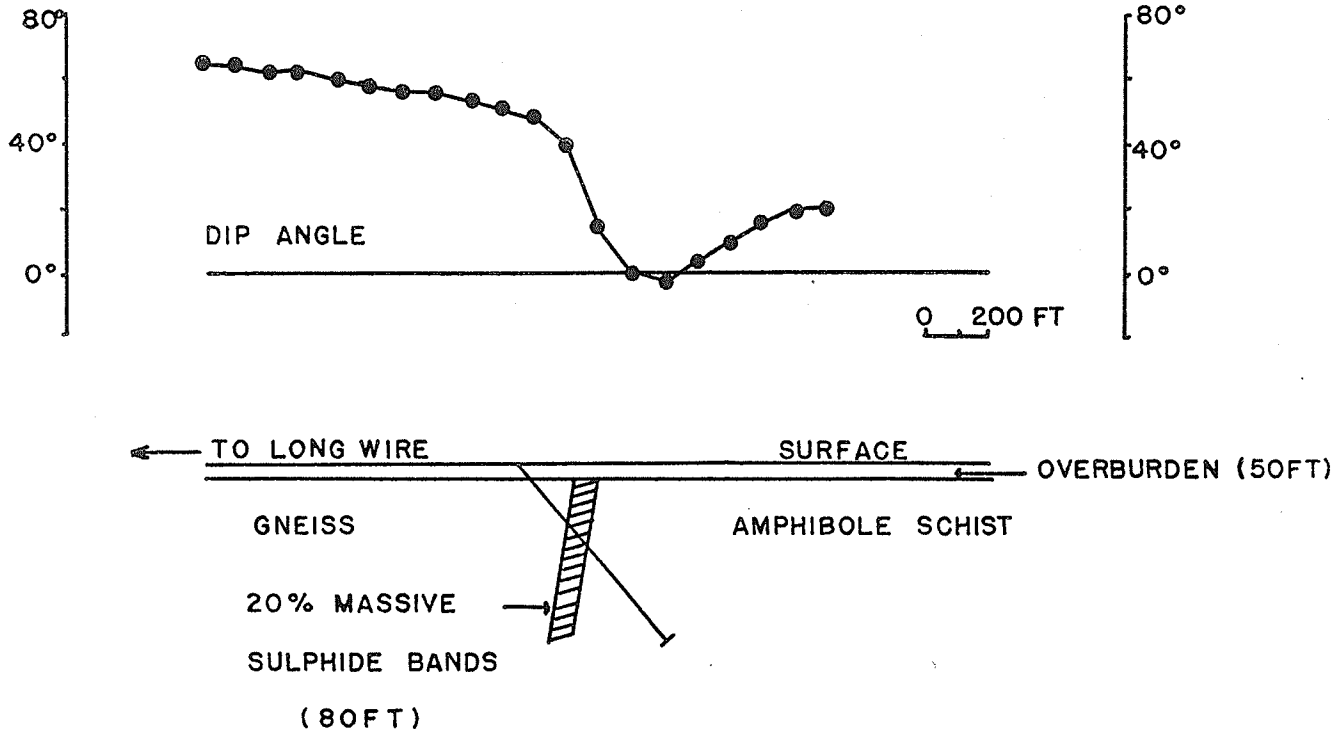

STRONG CONDUCTOR RESPONSE

Fig. 3. DPM-2 field measurements illustrating the peaks in the in-phase and quadrature components about the inflexion point in the dip angle profile (courtesy of Central Geophysics Limited).

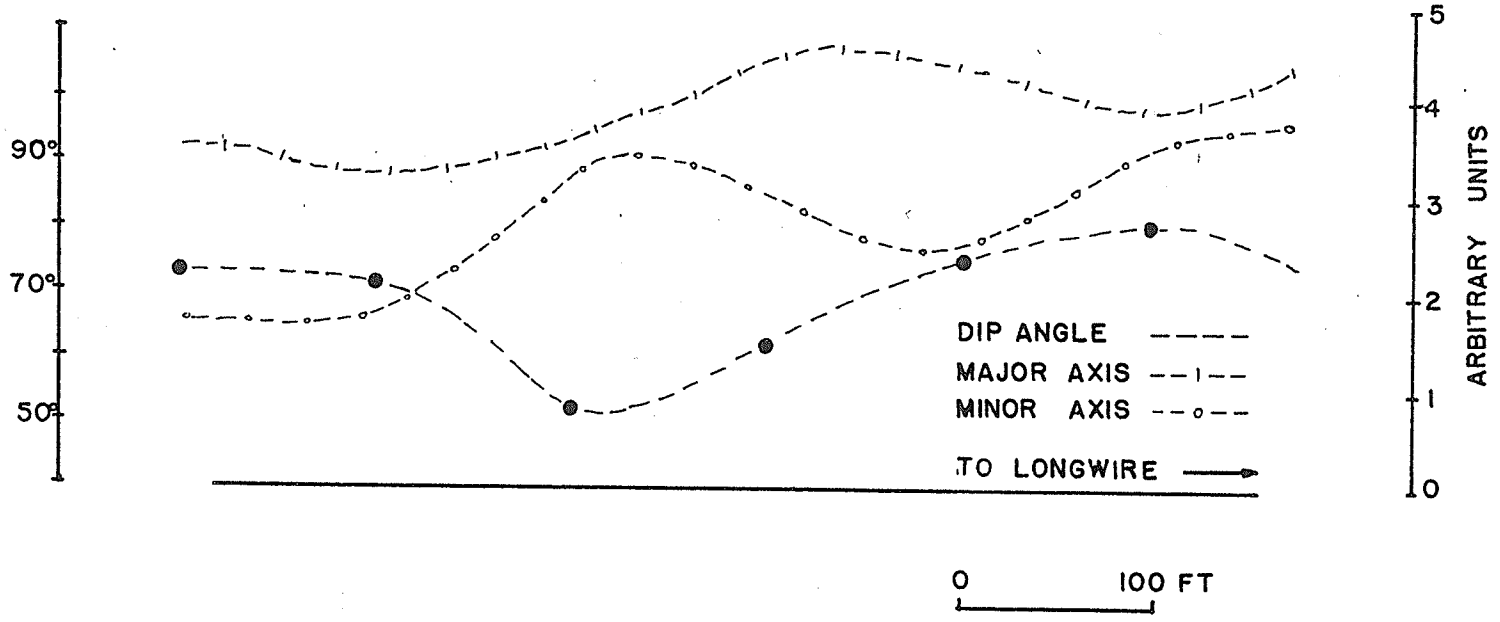

DPM - 2 RESPONSE

Fig. 4. Effects of a strong sferic background on the dip angle profile over a conducting body. The lines and stations in Figs. 4a and 4b are identical but the surveys were run on two different days. The dark line in Fig. 4a indicates that no reading could be taken at a station (courtesy Central Geophysics Limited).

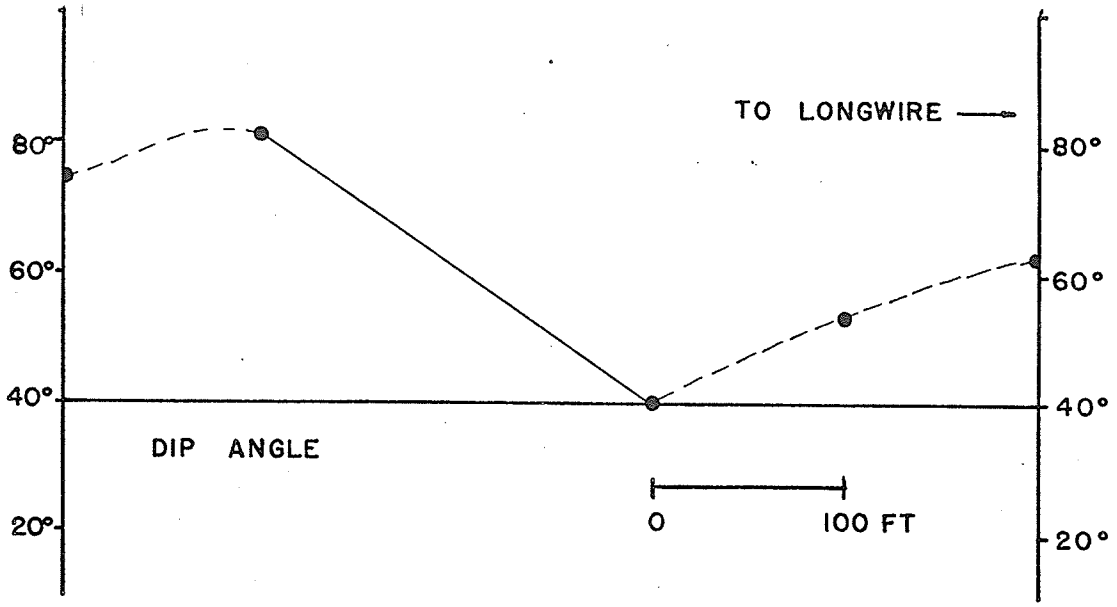

A

EFFECT OF STRONG SFERICS

ON DPM-I RESPONDER

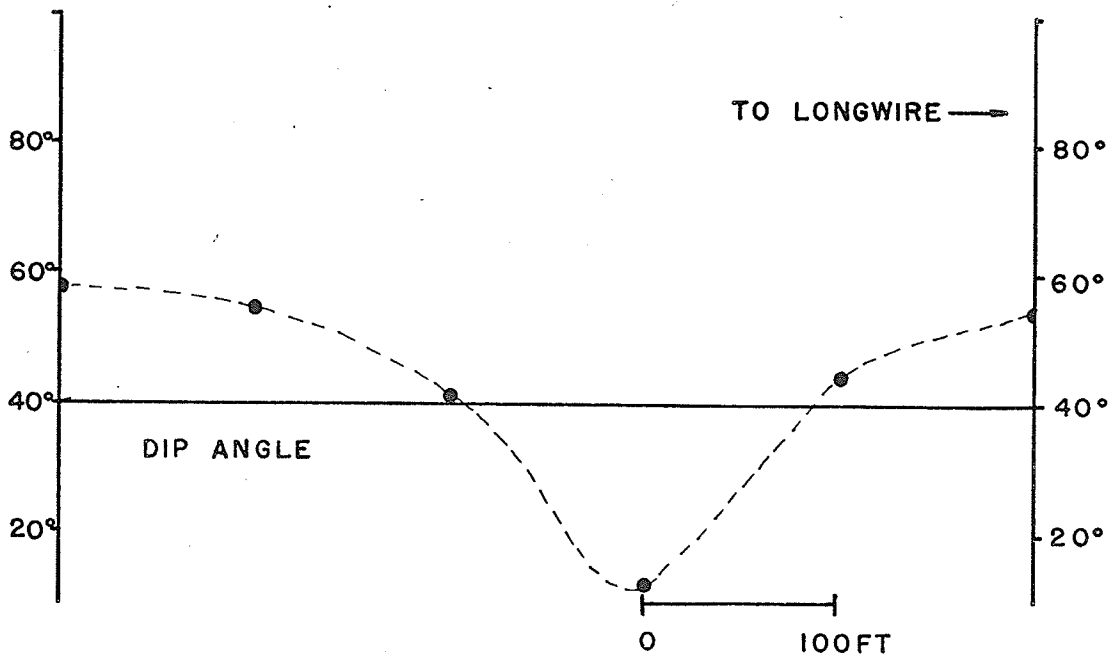

B

DPM-I RESPONDER

CHAPTER IV

INTERPRETATION

Although DPM-1 has been used for some hundreds of line miles, little work has been done in developing a formal interpretation scheme. Nevertheless, while not sophisticated, some general lines in interpretation have been followed, and have been quite successful in the locating of conductors.

The DPM-1 has also proven quite useful in making hidden lithologic boundaries fairly easy to discern. Owing to the fact that different rock units may have different electrical characteristics, the rate of fall-off in dip angle is a useful parameter to observe in order to follow structural trends. Figure 1 illustrates this well, where a factor of three in resistivity contrast almost doubles the rate of fall-off.

Fault or shear zones, either between differing rock units or otherwise, often have associated conducting mineralization or contain electrolytic solutions. They produce inflexions in the dip angle profile, and when of sufficient strike extent, may tend to channel return currents, making them easy to trace.

In areas with little outcrop, this ability to reflect

geologic structure is most useful.

From the economic standpoint, that of locating massive sulphides, interpretation has developed only as empirical (i.e. drill hole) results would allow. Conductor axis location is made by noting the point of inflexion (or minimum slope, as one moves away from the source), and depth to a body is suggested by anomaly width. The quality of the conductor is judged by the magnitude or vertical dimension of the anomaly. While these parameters may be valid, no formal studies have been made on their validity, and no firm guidelines exist for interpretation. For example, consider the case of finite depth extent. Some workers have suggested that the sudden rate of return in dip angle after passing over a conductive body such as that shown in Fig. 5, is due to finite depth extent. However, it can be seen that this may also be caused by a change in lithology. Still another cause might be a small and shallow conductor. It would be expected that this would have a localized or narrow anomoly of limited magnitude associated with it, because its size would reduce inductive coupling and hence the magnitude of eddy currents.

Another factor, whose effects will be pointed out later, and which affects the rate of return, is conductor quality. It will be seen that the poorer the quality, the more rapid the rate of return.

For the tilt angle method, quality is difficult to

Figure 5. DPM-1 profiles over the Uchi Lake ore zone illustrating the inductive response of the body by comparison of the surveys at different frequencies. Note that the shear zone responds at both frequencies implying that it is a conductive responder. (After Anderson and Sutherland, 1970)

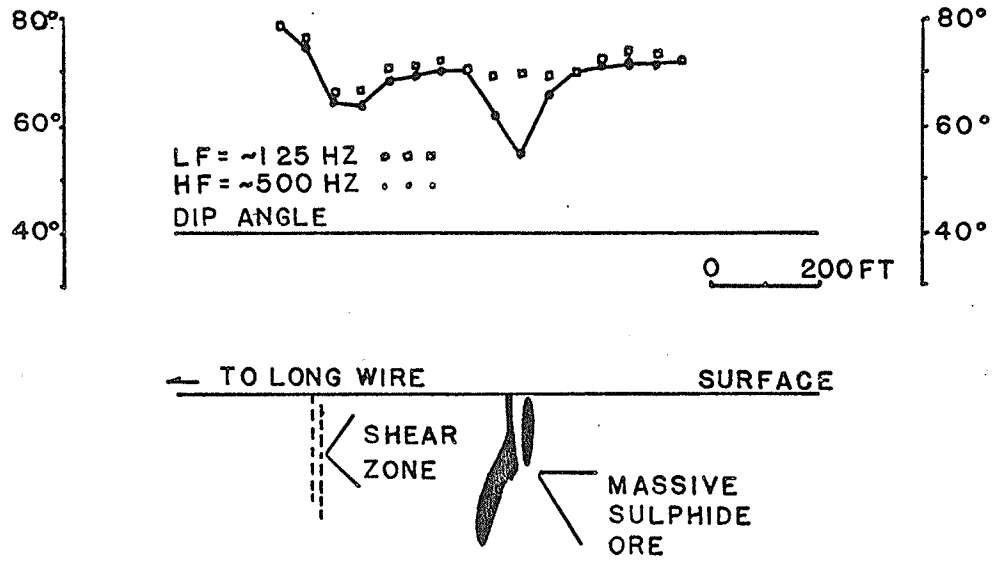

DPM - 1 RESPONSE AT TWO FREQUENCIES

assess from only one set of measurements at a single frequency. Only by using a multi-frequency survey can some estimate be made. This the case for many inductive systems, because the response is governed by a conductivity-frequency product (see Grant and West, p. 489). For the DPM-1 system surveys are generally run at only one frequency, hence, no quality estimates can be made. However, over the Uchi Lake ore zone, a second survey was run at a lower frequency. It can be seen though (Fig. 5), that the value chosen was too low to produce a measureable response for the conductivity and size of the body. All that may be concluded is that any measured response over the body is purely inductive, as it varied with the frequency. The DPM-2 system does not require multi-frequency surveys, however. It will be seen that the ellipticity of the field is a good measure of quality.

CHAPTER V

EXPERIMENTAL MODELS

Experimental modelling of electromagnetic prospecting systems can take two forms. One is the mathematical model, and the other, a physical model, either on a reduced lab scale, or at full scale, taking the form of a case history.

The mathematical analysis of EM responses is a difficult means of setting up an interpretation scheme. The mathematics is very complicated, and theoreticians are limited to obtaining solutions for only a few simple cases. For reason of simplification, assumptions concerning source-body configurations, the enclosing medium's size or electrical properties, or even the source or body dimensions, must be made (for example, see Hohman, 1970). Simplifications such as these, while permitting exact solutions, tend to restrict the applicability of the solutions when the characteristics of the geologic medium or responder depart greatly from the theoretical model.

Physical scale modelling permits a wider range of source-body geometries to be modelled and studied with greater ease. For the production of a useful interpretation scheme, where bodies may vary in size, shape, and electrical properties, or the source-body geometry may vary,

scale modelling is more versatile (for examples, see West, 1960, or Bosschart, 1964).

As a prelude to such a scale modelling study and in conjunction with instrument development, a ribbon-current model study, to be described presently, was instituted. Its object was to produce curves of the form that would be observed by the field instrument being developed, and to examine their characteristics with the view to proposing the form of a basic interpretation scheme to estimate depth and conductor quality. While only a very simple model, it was hoped that the results might also be useful in assessing instrument performance, and the future model performance.

CHAPTER VI

BASIC THEORY

Phase Relationships

The basic assumptions made for the ribbon-current model were that those eddy currents in a near-vertical, sheet-like conductor, most effective in producing measured anomalies may be presumed to be located at some fixed depth and have the form of a finite current concentration or line source. In addition, this line current might be determined in magnitude by the characteristics of the field at the ground surface. This corresponds to what other workers (Parasnis, 1966; Keller and Frischknecht, 1966) suggest as an approximation to such a responding body. This is equivalent to saying that the conductor could be modelled as a very large square loop in a uniform field, and that the effects of the vertical arms and the bottom were negligible.

It is not presumed that this is an accurate model, but the fact that a reasonable fit was made to a known conductor in an apparently electrically homogeneous ground, suggests that even though very simple, under certain conditions, it is not an unsatisfactory one.

From Faraday's law, the potential induced in a loop circuit may be expressed as:

$$V_1 = -i\omega M I_o e^{i\omega t} \qquad \ldots 5$$

where

ω = radial frequency

M = coefficient of mutual inductance

I_o = source current amplitude

t = time

If a current $I_1 e^{i\omega t}$ flows in the loop circuit, then there must be a potential drop due to the ohmic resistance and the self inductance. This back potential may be expressed as:

$$V_\beta = -(R + i\omega L) I_1 e^{i\omega t} \qquad \ldots 6$$

where

R = ohmic resistance

L = self inductance

I = amplitude of the loop current

Kirchoff's laws require that the sum of all potentials in a circuit loop be zero. Hence,

$$V_\beta - V_1 = 0 \qquad \ldots 7$$

$$i\omega M I_o e^{i\omega t} - (R + i\omega L) I_1 e^{i\omega t} = 0 \qquad \ldots 8$$

$$I_1 e^{i\omega t} = \frac{-i\omega M I_o e^{i\omega t}}{(R + i\omega L)} \qquad \ldots 9$$

$$I_1 = \frac{-\omega M I_o (\omega L + iR)}{(R^2 + \omega L^2)} \qquad \ldots 10$$

where the real and imaginary parts combine to result in a net phase shift of:

$$\alpha^1 = \pi + \tan^{-1}\left(\frac{R}{\omega L}\right) = \pi + \alpha \qquad \ldots 11$$

where

α = conductor quality with low values denoting better quality.

It is evident that an ideal conductor would have secondary currents exactly in opposition with the source current, or correspondingly, exactly in phase with return currents. The poorest conductors, would have currents approaching 90° out of phase with source currents, and would follow them by that amount. Lamontagne and West's (1970) results demonstrate this for planar conductors in the field of a large horizontal loop.

It was noted earlier that for a sufficiently wide electrode spacing secondary currents are predominantly induced. For a uniform country rock, return currents are distributed in a manner characteristic of two point electrodes on a uniform halfspace, the current density diminishing as the inverse second power of the distance from the electrodes. More-conductive zones will tend to bias the return current paths, the current density being greater in these regions. How much of an effect this current has on

anomalies may be seen in a qualitative way, for this model.

Suppose that there exists a unit induced current differing in phase with the primary current by an amount 'α', the phase angle of equation 11. If some return current 'I' is carried by the ribbon, then the result will be a current differing in phase and magnitude with both components. This may be described as follows:

$$I'[\sin(\omega t+\alpha+\theta)] = I[\sin(\omega t)] + I''[\sin(\omega t+\alpha)] \quad \ldots 12$$

where

I' = amplitude of the resultant current

θ = additional phase angle due to current summation

I = amplitude of the return current

I'' = unit induced current amplitude

By expansion of trigonometric functions, it may be deduced that:

$$I'[\cos(\alpha+\theta)] = I + I''[\cos(\alpha)] \quad \ldots 13$$

and

$$I'[\sin(\alpha+\theta)] = I''[\sin(\alpha)] \quad \ldots 14$$

Thus, the return current enhancing the conductor quality by an amount 'θ' is:

$$I = \frac{\sin(\alpha)}{\tan(\alpha+\theta)} - \cos(\alpha) \quad \ldots 15$$

and the amplitude of the resultant current is:

$$I' = [(1 + \cos(\alpha))^2 + \sin^2(\alpha)]^{\frac{1}{2}} \quad \ldots 16$$

Table I shows the effects of a conductor enhancement of 5^{o} by passing return current along the conductor axis. For this model it is evident that return currents would have to form a large percentage of the total current to enhance the quality of an excellent conductor by very much. For poorer bodies, the percentage decreases considerably. However, unless a body is near one electrode, it is not likely that the return current density in the region of the body will be sufficiently large to effect a significant change in response. The Uchi Lake ore zone in Fig. 5 is an example.

Field Representation

Bezvoda noted that the magnitude of the major and minor axes of the magnetic field ellipse varied with the conductivity of the host rock and the displacement from the source. In his presentation (Fig. 1) the major axis was normalized to 1.0 at the source, and decreased in value away from the source. For purposes of comparing computed and field anomalies, this is not suitable, because the ambient field would be some fraction of 1. Hence, it was assumed that the size of the major axis of the ambient field had the value of 1.0 at any point of measurement. The value of the minor axis was then set at some fraction of this, depending on the current dip angle. By simply dividing the measured in and out-of-phase values by the normal field in-phase, computed

Table I

Conductor Enhancement

True Quality	Enhanced Quality	Return Current / Induced Current	Resultant Current	% Return / Return+Induced	% Return / Resultant
10^{o}	5^{o}	.999	1.990	49.9	50.2
20^{o}	15^{o}	.336	1.319	25.1	25.4
30^{o}	25^{o}	.205	1.181	17.0	17.3
40^{o}	35^{o}	.150	1.082	13.0	13.8
50^{o}	45^{o}	.123	1.082	10.9	11.3
60^{o}	55^{o}	.106	1.056	9.5	10.0
70^{o}	65^{o}	.095	1.035	8.6	9.1
80^{o}	75^{o}	.089	1.018	8.1	8.7

and measured anomalies might easily be compared.

For some dip angle 'β', that is, the angle between the major axis and the horizontal, the source field was described as follows,

$$\text{Source Field} = -A\cdot\sin(\omega t)\cos(\beta)\hat{i} - C\cdot\cos(\omega t)\sin(\beta)\hat{i}$$
$$-A\cdot\sin(\omega t)\sin(\beta)\hat{j} + C\cdot\cos(\omega t)\cos(\beta)\hat{j} \quad \ldots 17$$

where

A = length of the major axis

C = length of the minor axis

and is pictured in Fig. 6.

The field of the ribbon current varies inversely as the distance from the current and also differs in phase with the source current. This secondary field may be described by,

$$\frac{\vec{K}\cdot\sin(\omega t+\alpha)\ x\ \hat{r}}{r} = \vec{B}\cdot\sin(\omega t+\alpha)\ x\ \hat{r} \quad \ldots 18$$

where

$\vec{K}$ = scale factor involving current

r = distance from the source

α = phase angle

$\hat{r}$ = unit vector in the radial direction

and is also pictured in Fig. 6.

The resulting field is described by:

$$\vec{R} = (-\cos(\beta)\sin(\omega t) - C\cdot\sin(\beta)\cos(\omega t) - B\cdot\cos(\theta)\sin(\omega t+\alpha))\hat{i}$$
$$+(-\sin(\beta)\sin(\omega t) + C\cdot\cos(\beta)\cos(\omega t) + B\cdot\sin(\theta)\sin(\omega t+\alpha))\hat{j} \quad \ldots 19$$

Fig. 6. Field representation for computing responses over the ribbon model illustrating the summation of primary and secondary field vectors to produce the resulting dip angle profile.

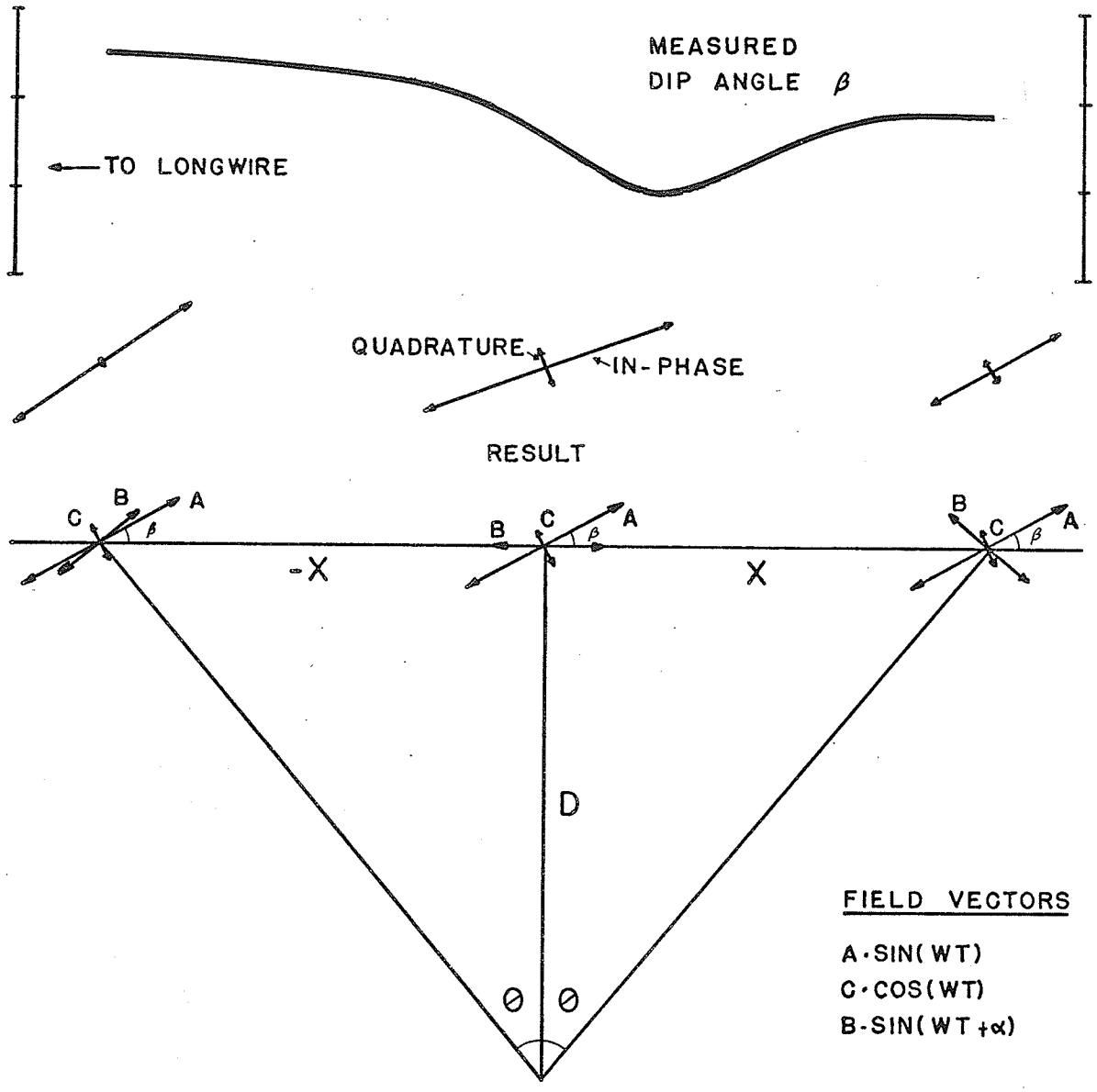

RIBBON SOURCE

By finding the maximum and minimum of $\vec{R}$ of $|\vec{R}|^2$ in time, the values of both major and minor axes can be calculated for various values of 'α' and 'r'. Knowing the time that the field vector is oriented along the major axis allows a determination of the dip angle. It is given by the arctangent of the ratio of the $\hat{j}$ and $\hat{i}$ components of $\vec{R}$.

For purposes of comparing computed and measured anomalies, all distances must be in the same units. As easily measured parameter, to which all might be related would be useful. A fairly obvious unit, the one chosen, is skin depth 'δ', a parameter related to the conductivity of the host rock, and hence which must have a bearing on the conductor's response.

It will be recalled that the rate of fall-off in dip angle is affected by the host rock's conductivity. Hence, by noting the changes in dip angle, 'δ' can be estimated. Its effect on the response of a body depends on the depth fraction of 'δ', that is, identical bodies in two homogeneous hosts of differing conductivities, would have identical responses if the depths to the bodies, in terms of skin depth, were equal. For example, if the hosts had 'δ' values of 2000 ft and 4000 ft respectively and the bodies were at depths of 500 ft and 1000 ft, the dip angle being the same at each location, the magnetic fields inducing eddy currents in the bodies would be the same. Hence, the

measured responses would be the same, providing that the horizontal scale was a fraction of skin depth as well. However, for a sufficiently large skin depth and shallow enough body, it would be expected that changes in 'δ' would not produce measureable changes in the response. Therefore, a fixed, but arbitrary reference might be chosen. However, for this study, the skin depth was of the order of 2000 ft and for the depths of interest, (up to 500 ft), it was felt that the resulting depth fraction (.25) was too large for a fixed reference of only 2000 ft. If 'δ' increased to 2500 ft in some other area, the maximum depth fraction of 0.25 would represent 625 ft. Consequently, presented results were left in terms of depth fraction.

A FORTRAN IV program (Appendix I) was written to calculate anomalies under a variety of conditions. It listed characteristics of the data and plotted the results.

CHAPTER VII

RESULTS

The program described in Appendix I permitted the plotting of calculated anomalies on graphs up to 6 x 10 inches in size, with plotting increments of 0.1 inches. Consideration was made for the variation of dip angle and quadrature component of the source field for a survey line of variable length. While no scale factor change was made for variation in conductor quality or depth, changes in scale factor were made for different positions of the body (i.e. source body distance). These were based on changes in the component of the major axis normal to the body, which were found comparable to the horizontal component of the vector R and the component of the average value of R normal to the conductor (see Fig. 7).

To test the model, a field curve that seemed typical of an electrically uniform host rock containing a near vertically oriented conducting body was chosen. From those available to the writer, Fig. 7 of Anderson and Sutherland's (1970) paper was the only suitable curve.

An estimate of skin depth yielded a value near 2000 ft., with an ambient dip angle of 40°. By varying the depth and scale factor, and making a small change in the ambient dip

Fig. 7. The component of the major axis of the primary field ellipse normal to the body for a vertically uniform field as a function of distance from the source.

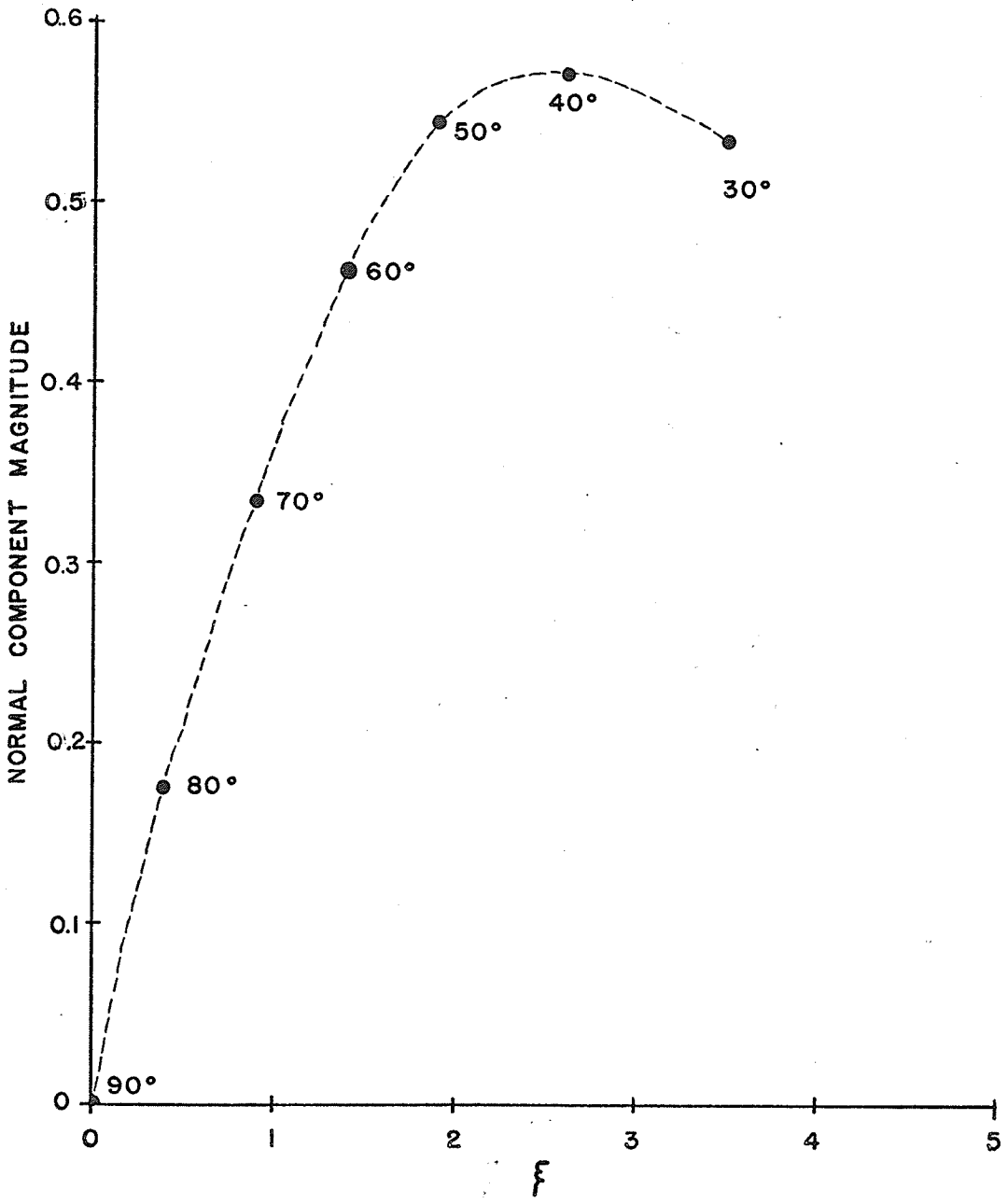
NORMAL COMPONENT MAGNITUDE
0.6
0.5
0.4
0.3
0.2
0.1
0
0
1
2
3
4
5
ξ
90°
80°
70°
60°
50°
40°
30°

angle, a fit was made to the field data within the 2^{o} error quoted in their paper, by a computed anomaly at an ambient dip angle of 42^{o}, a depth of 0.0878 (~175 ft) and with a scale factor of 0.1195. The comparison with the computed anomaly (see Fig. 8) indicated that the conductor had not only strong eddy currents but was of good quality as well. Accompanying Figs. 9, 10, and 11 are the associated in-phase, out-of-phase and ellipticity curves.

This fit to field data indicated that the model was not an unreasonable one.

Using the estimated changes for the scale factor with the distance from the source, Figs. 12 to 19 were produced for dip angles of 60^{o} and 80^{o}, for a depth of 0.087. For the assumptions made about the uniformity of the field with depth, these would be typical of a strong conductor response nearer the source cable.

The dip angle curves seem revealing of conductor quality. The minimum dip angle decreases while the rate of return to the norm increases with decreasing quality.

This observation suggested that the Uchi Lake body might be of poor quality, but attempts to fit curves to the data were fruitless and lead to the conclusion that the rapid rate of return to the norm were due more to geology than quality.

Curves for in-phase and quadrature vary with quality in opposite manners, the former decreasing and the latter

Fig. 8. Computed dip angle profiles at 10^{o} increments of phase angle illustrating the fit to Anderson and Sutherland's strong conductor.

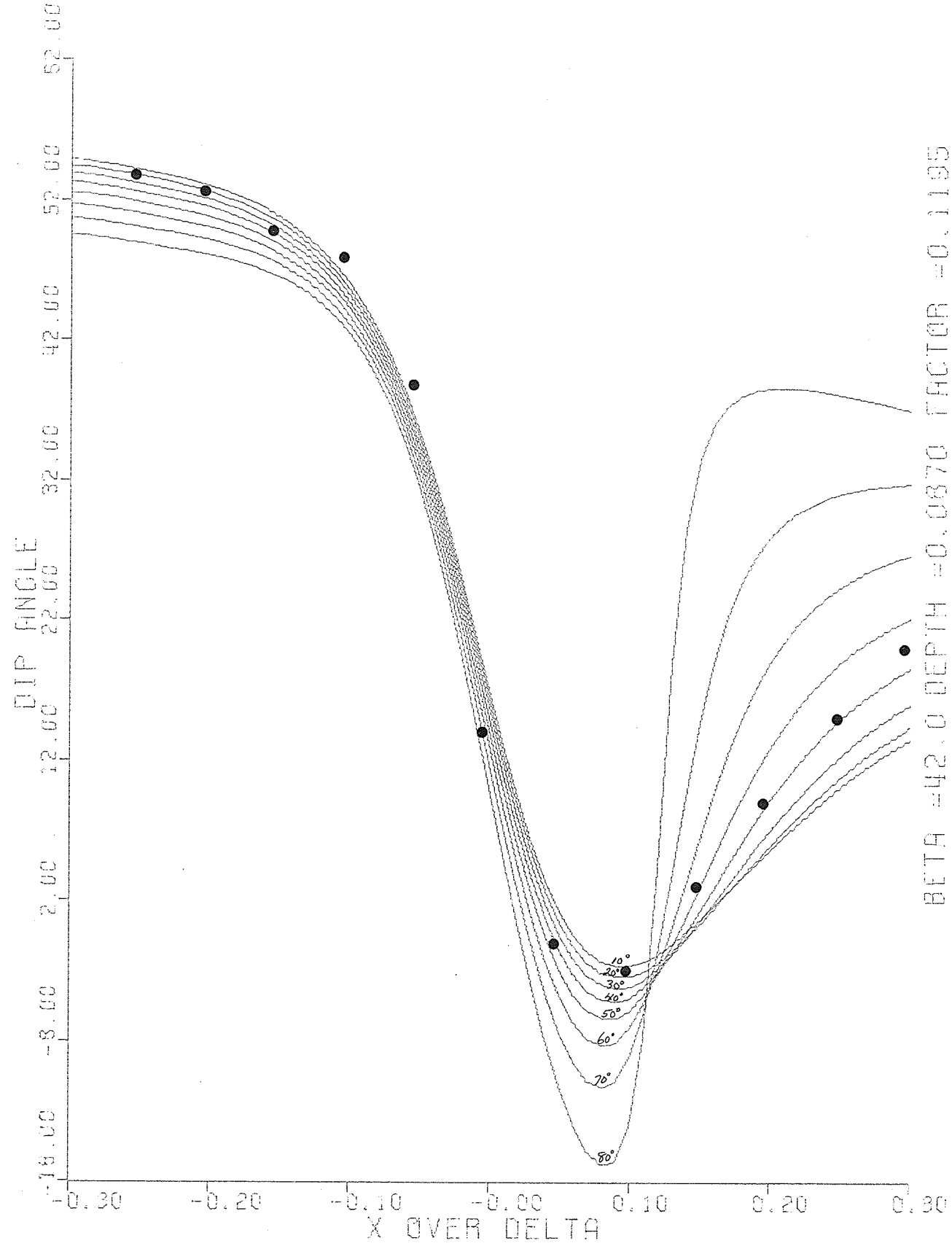
DIP ANGLE
52.00
42.00
32.00
22.00
12.00
2.00
-8.00
-18.00
-0.30
-0.20
-0.10
-0.00
0.10
0.20
0.30
X OVER DELTA
10°
20°
30°
40°
50°
60°
70°
80°
BETA =42.0 DEPTH =0.0870 FACTOR -0.1195

Figs. 9, 10, and 11. Associated in-phase, quadrature and ellipticity curves for the dip angle profiles of Fig. 8, which illustrates the fit to Anderson and Sutherland's strong conductor.

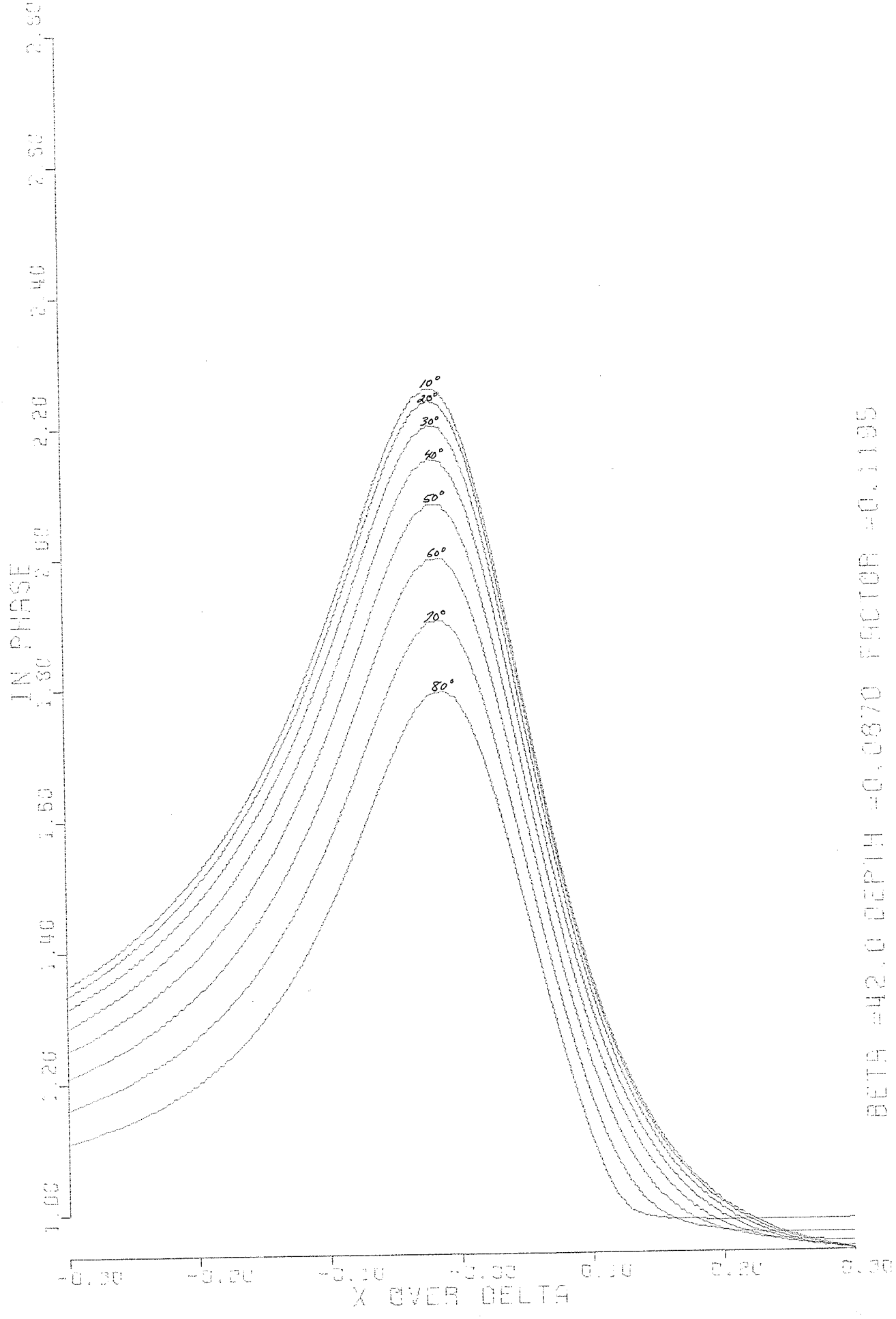
IN PHASE
X OVER DELTA
BETA =42.0 DEPTH =0.0870 FACTOR =0.1195
10°
20°
30°
40°
50°
60°
70°
80°

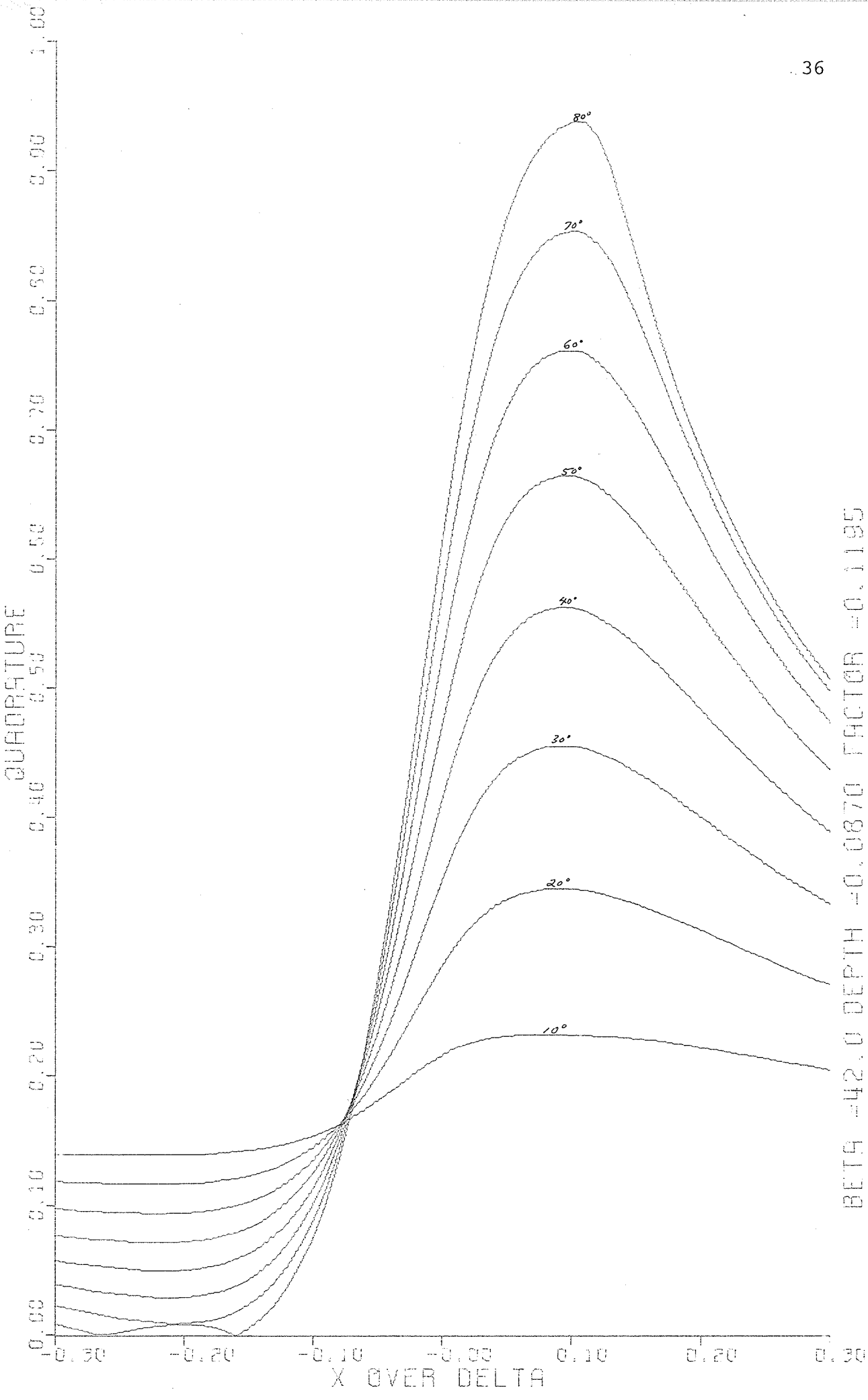
80°
70°
60°
50°
40°
30°
20°
10°
QUADRATURE
0.00
0.10
0.20
0.30
0.40
0.50
0.60
0.70
0.80
-0.30
-0.20
-0.10
-0.00
0.10
0.20
0.30
X OVER DELTA
BETA -42.0 DEPTH -0.0870 FACTOR -0.1195

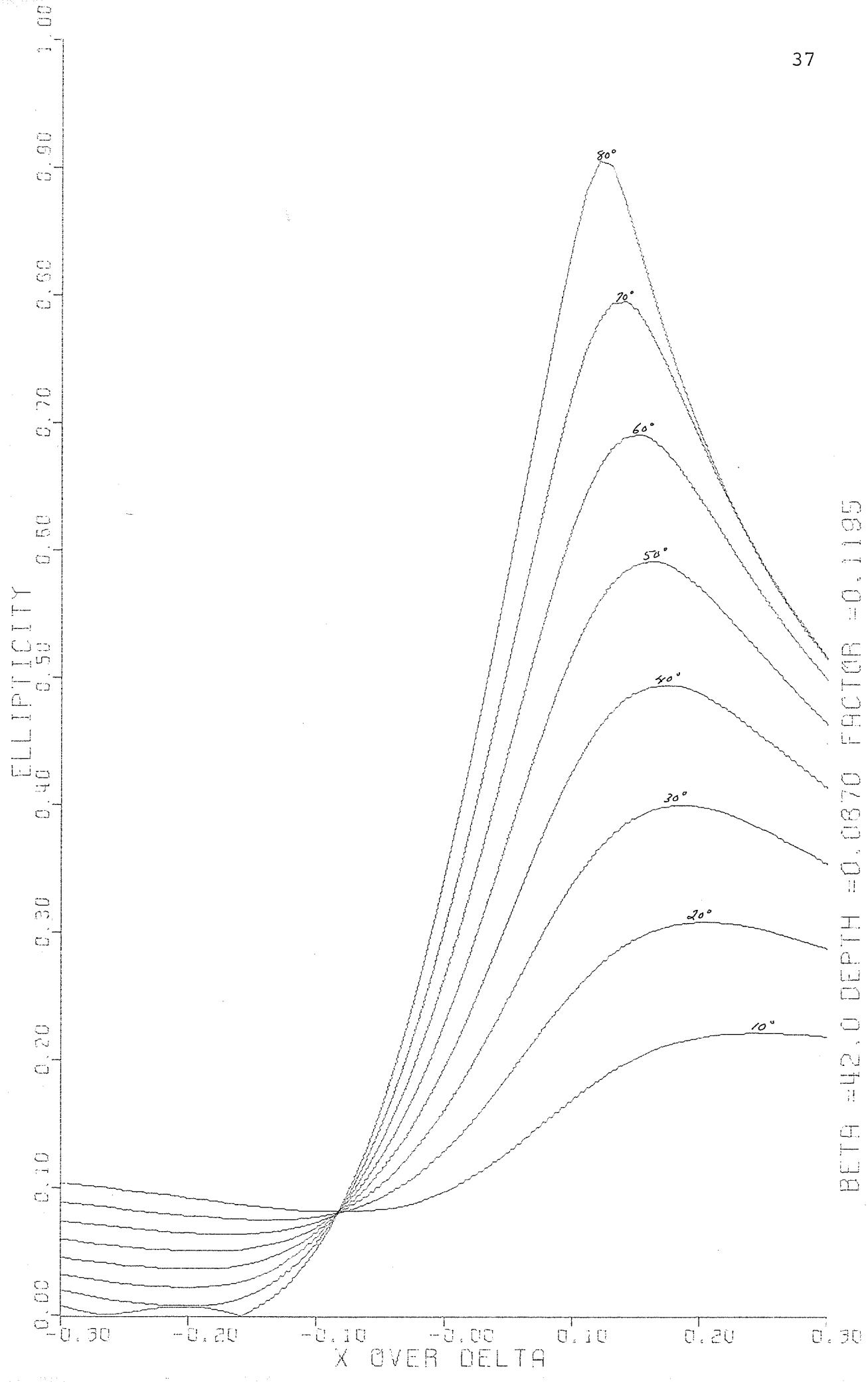
ELLIPTICITY
0.00
0.10
0.20
0.30
0.40
0.50
0.60
0.70
0.80
0.90
1.00
-0.30
-0.20
-0.10
-0.00
0.10
0.20
0.30
X OVER DELTA
80°
70°
60°
50°
40°
30°
20°
10°
BETA =42.0 DEPTH =0.0870 FACTOR =0.1195

Figs. 12, 13, 14, and 15. Dip angle, field component and ellipticity profiles for a strong conductor at an ambient primary dip angle of 60°, based on Anderson and Sutherland's strong conductor.

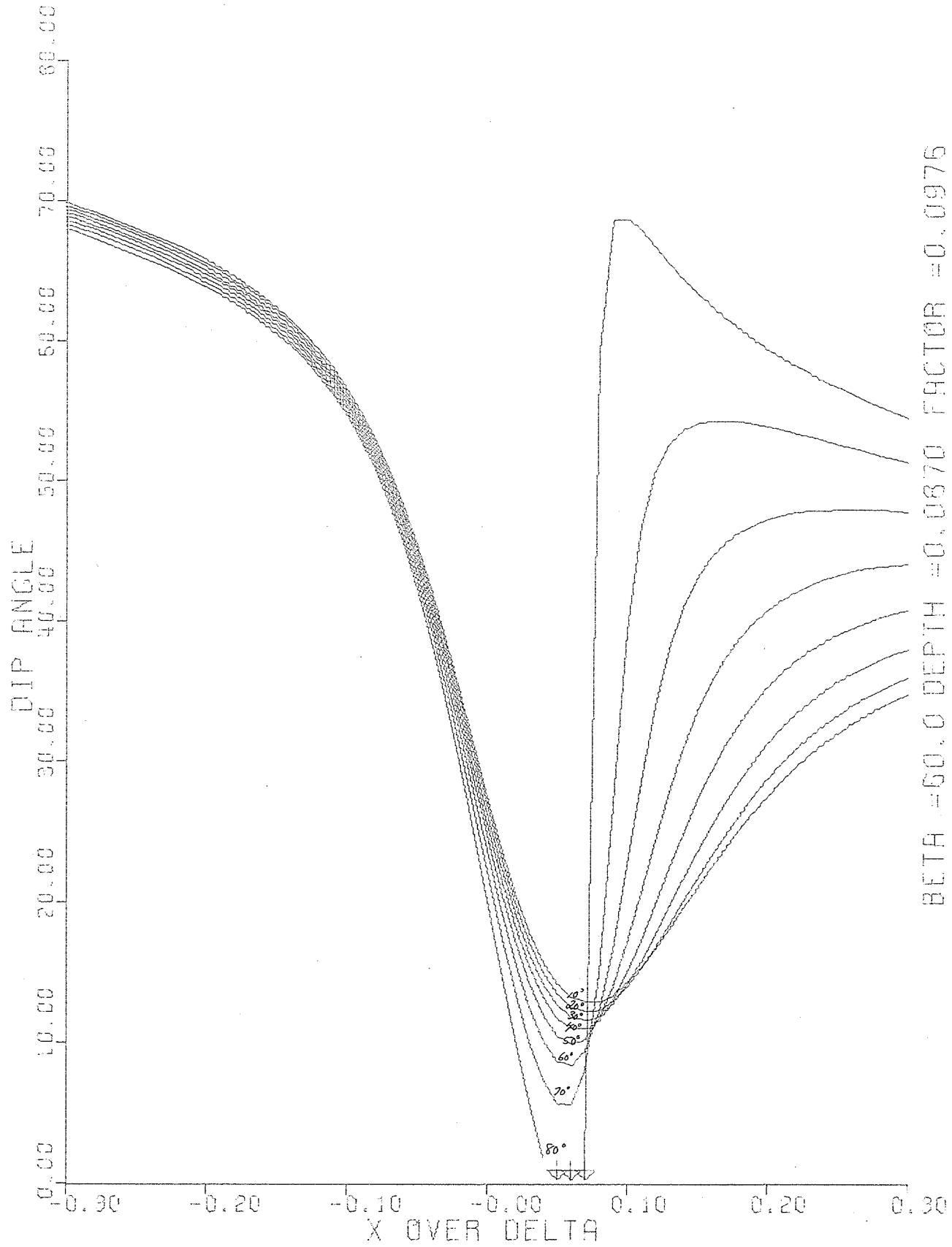
DIP ANGLE
0.00
10.00
20.00
30.00
40.00
50.00
60.00
70.00
80.00
-0.30
-0.20
-0.10
-0.00
0.10
0.20
0.30
X OVER DELTA
10°
20°
30°
40°
50°
60°
70°
80°
BETA =60.0 DEPTH =0.0870 FACTOR =0.0975

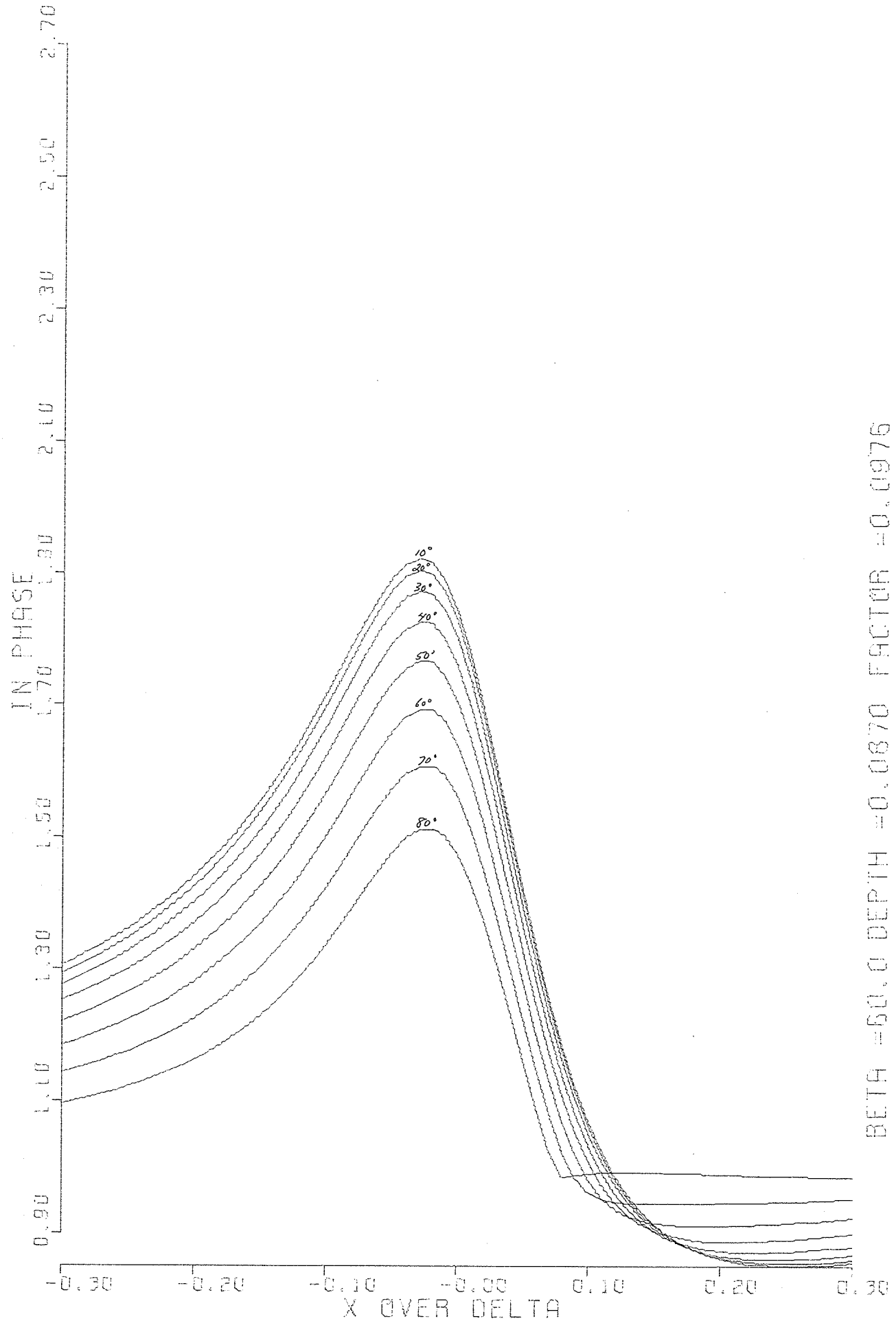
IN PHASE
0.90
1.10
1.30
1.50
1.70
1.90
2.10
2.30
2.50
2.70
10°
20°
30°
40°
50°
60°
70°
80°
-0.30
-0.20
-0.10
-0.00
0.10
0.20
0.30
X OVER DELTA
BETA =60.0 DEPTH =0.0870 FACTOR =0.0976

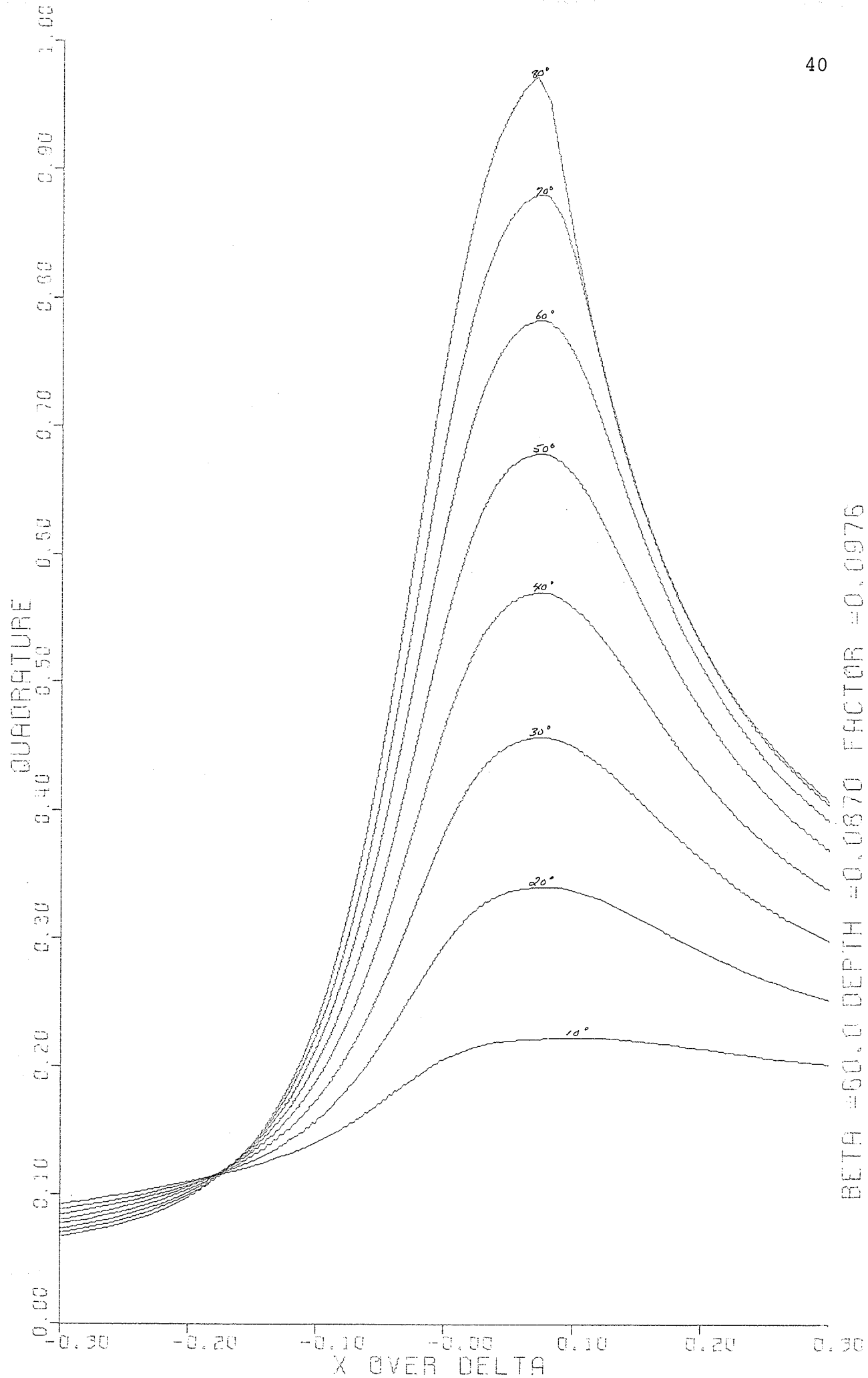
QUADRATURE
0.00
0.10
0.20
0.30
0.40
0.50
0.60
0.70
0.80
0.90
1.00
-0.30
-0.20
-0.10
-0.00
0.10
0.20
0.30
X OVER DELTA
80°
70°
60°
50°
40°
30°
20°
10°
BETA =60.0 DEPTH =0.0870 FACTOR =0.0976

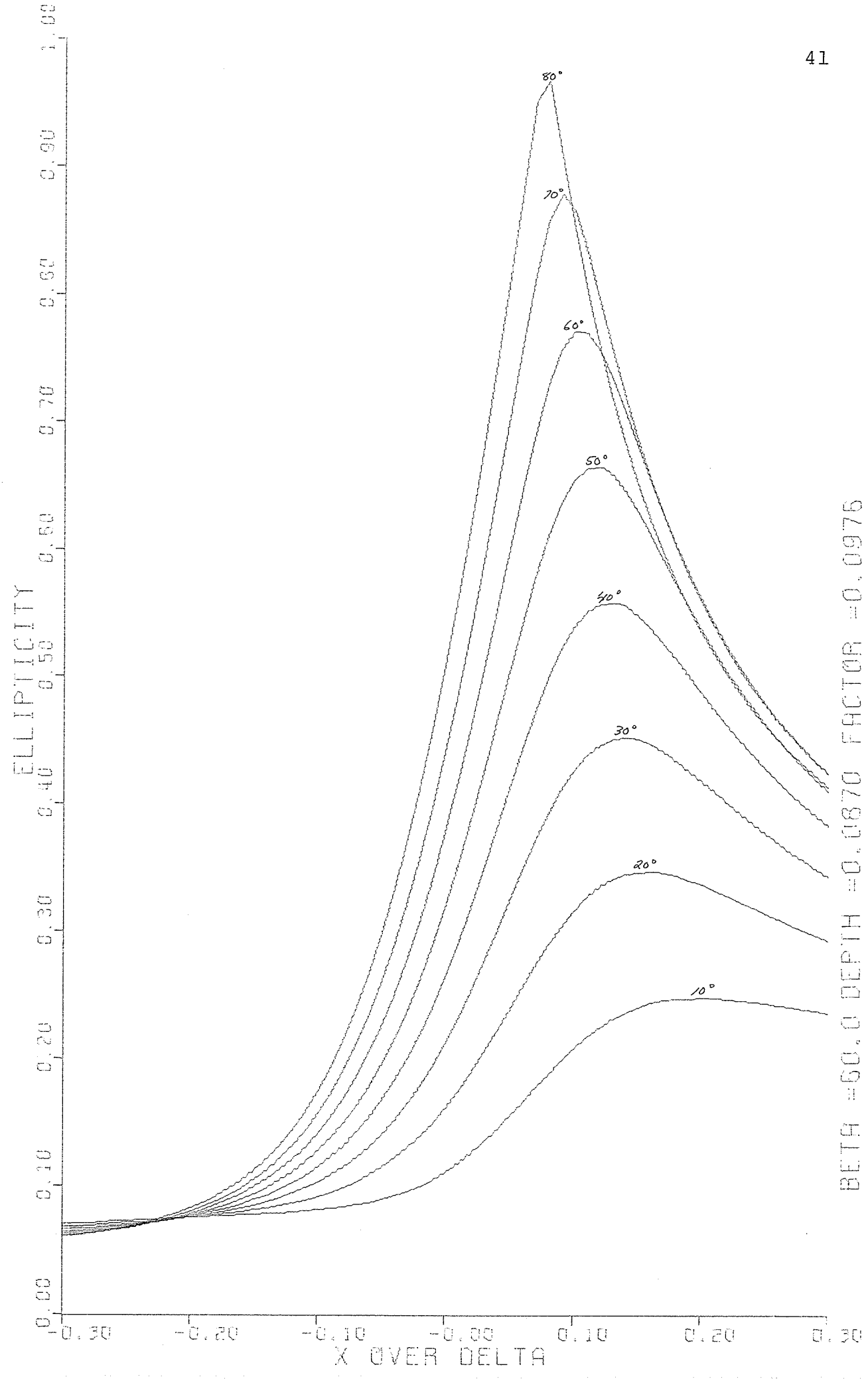
ELLIPTICITY
0.00
0.10
0.20
0.30
0.40
0.50
0.60
0.70
0.80
0.90
1.00
-0.30
-0.20
-0.10
-0.00
0.10
0.20
0.30
X OVER DELTA
80°
70°
60°
50°
40°
30°
20°
10°
BETA =60.0 DEPTH =0.0870 FACTOR =0.0975

Figs. 16, 17, 18, and 19. Dip angle, field component and ellipticity profiles for a strong conductor at an ambient primary field dip angle of 80^{o}, based on Anderson and Sutherland's strong conductor.

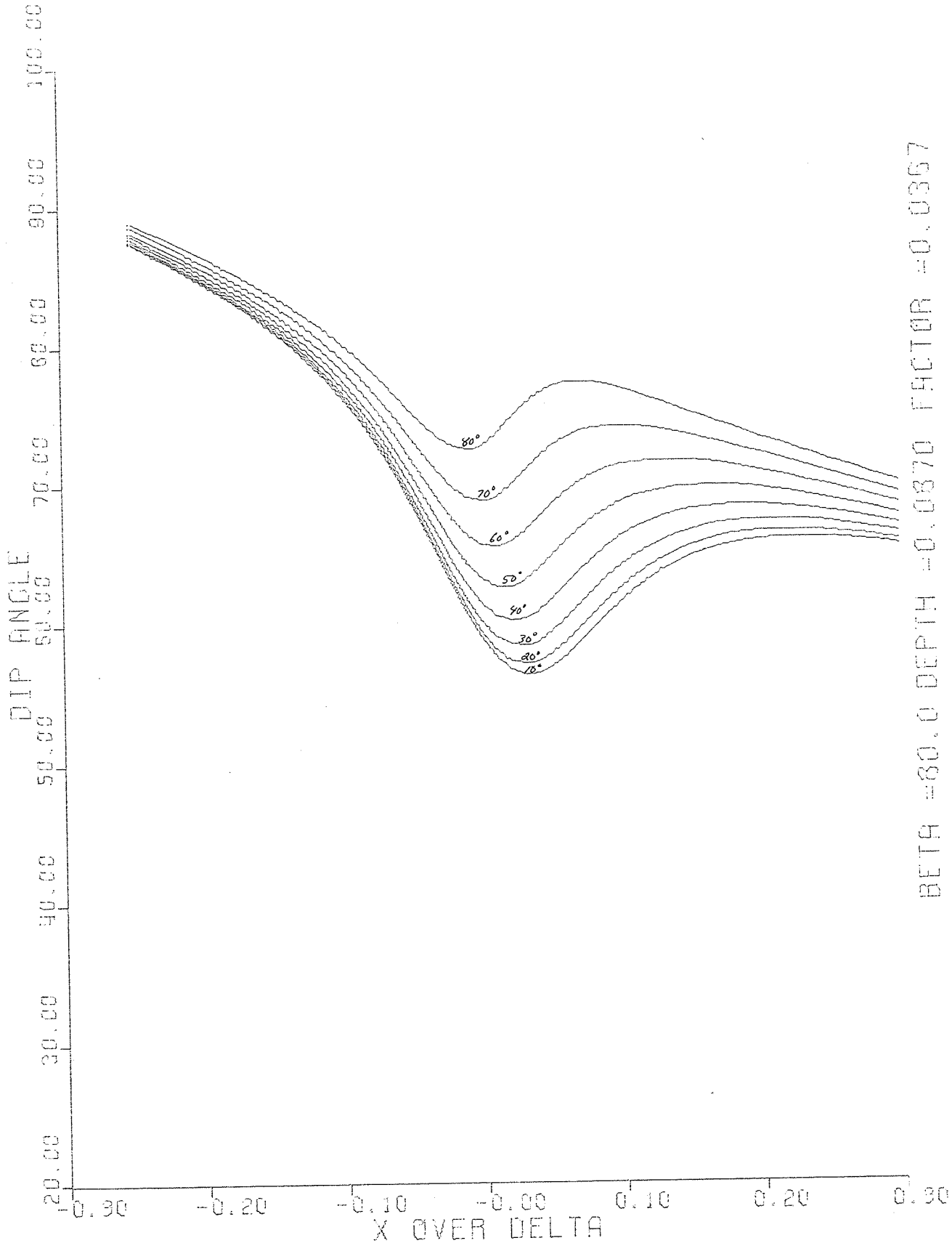
DIP ANGLE
20.00
30.00
40.00
50.00
60.00
70.00
80.00
90.00
100.00
-0.30
-0.20
-0.10
-0.00
0.10
0.20
0.30
X OVER DELTA
80°
70°
60°
50°
40°
30°
20°
10°
BETA =80.0 DEPTH -0.0370 FACTOR -0.0357

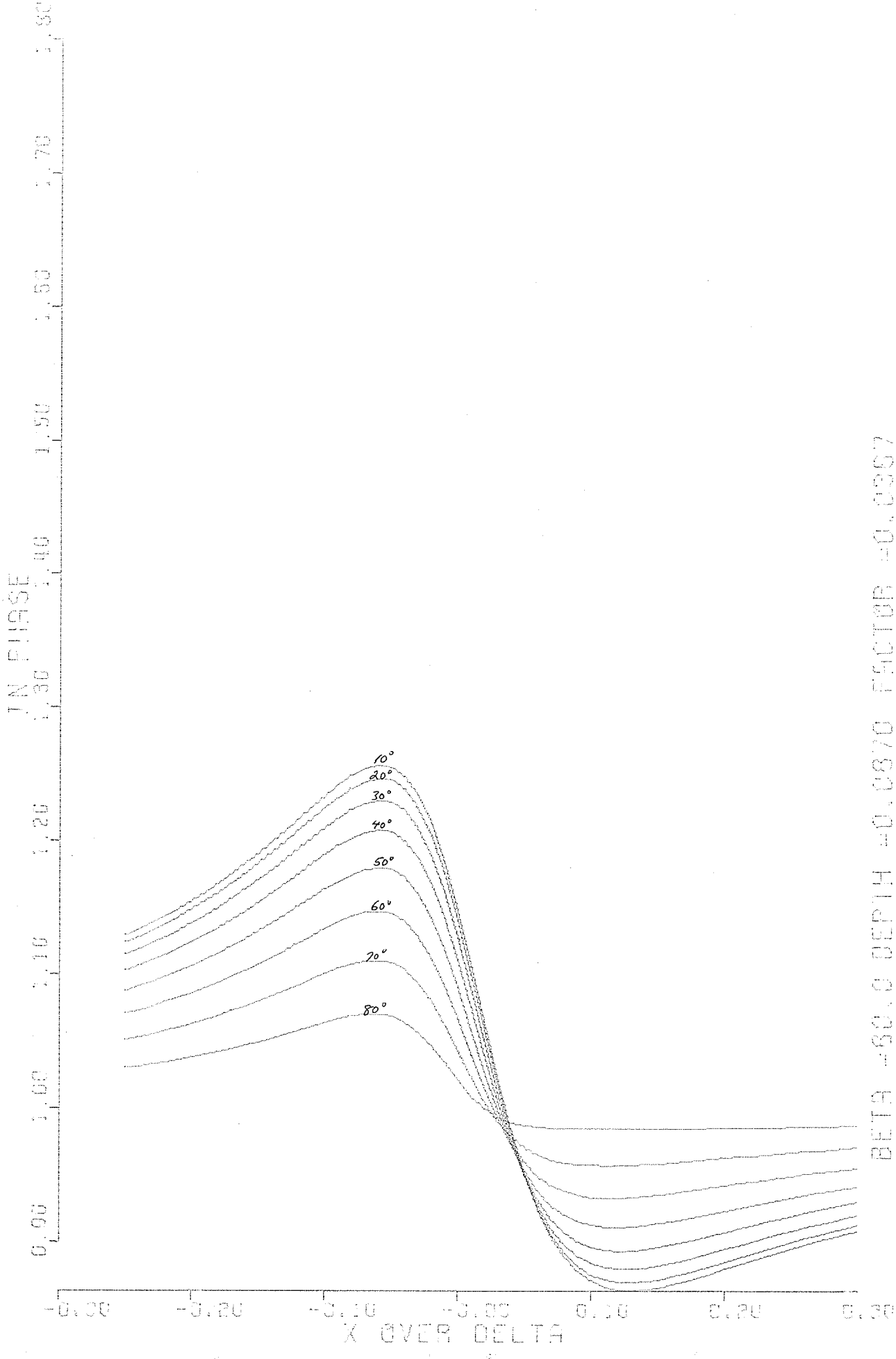
IN PHASE
0.90
1.00
1.10
1.20
1.30
1.40
1.50
1.60
1.70
1.80
10°
20°
30°
40°
50°
60°
70°
80°
-0.30
-0.20
-0.10
-0.05
0.10
0.20
0.30
X OVER DELTA
BETA -80.0 DEPTH -0.0870 FACTOR -0.0867

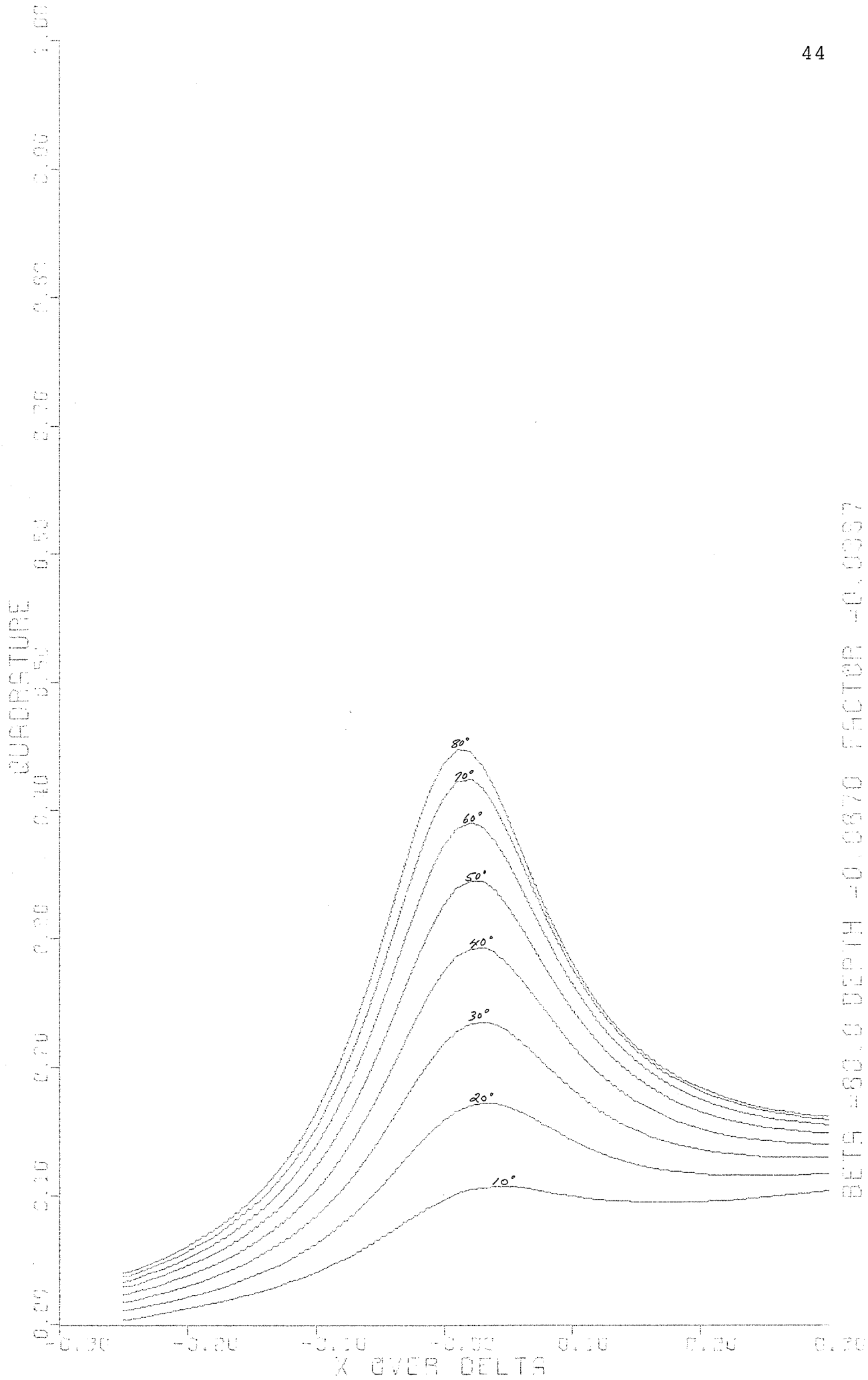
QUADRATURE
X OVER DELTA
BETA -90.0 DEPTH -0.6870 FACTOR -0.0007
80°
70°
60°
50°
40°
30°
20°
10°

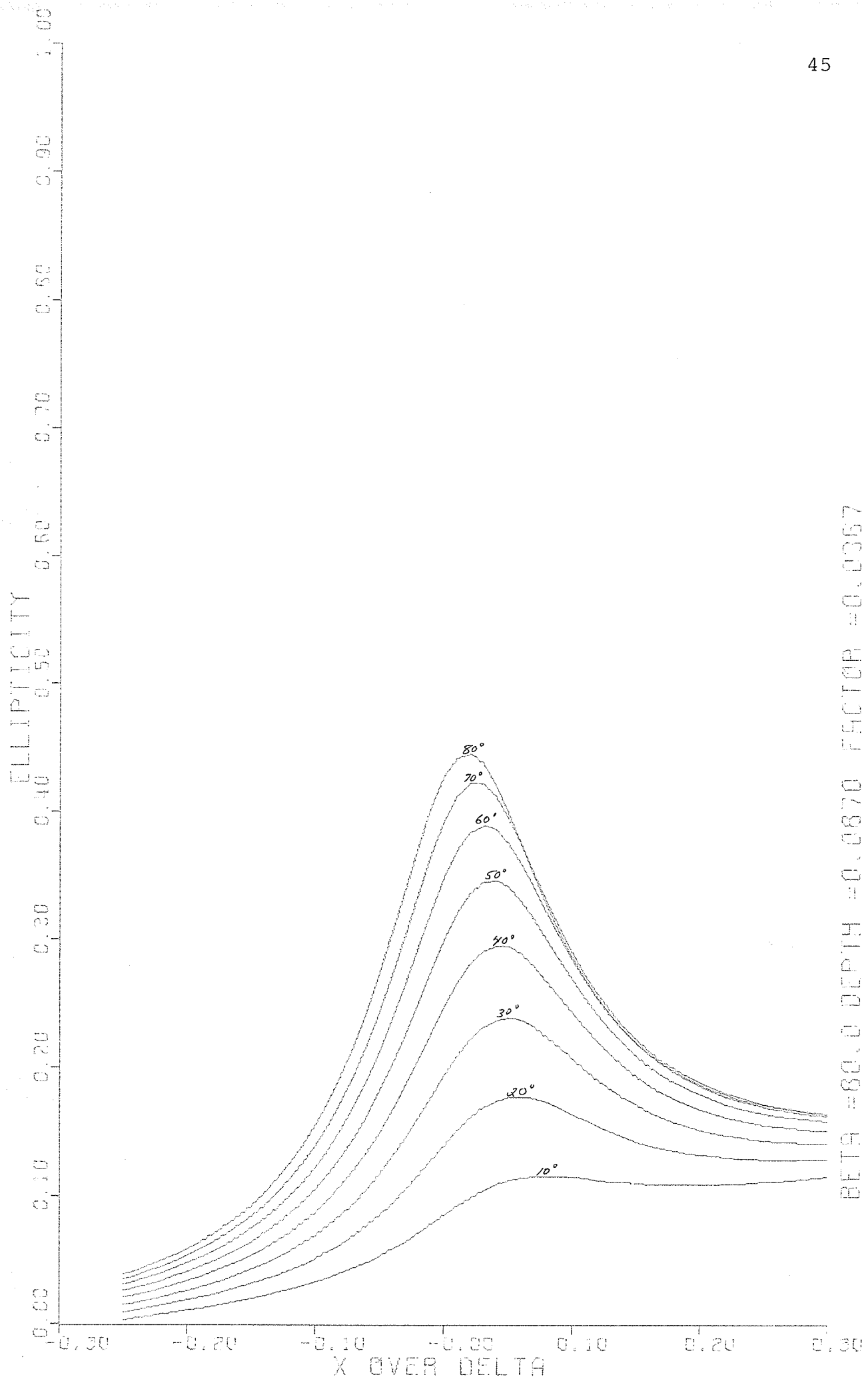
ELLIPTICITY
0.00
0.10
0.20
0.30
0.40
0.50
0.60
0.70
0.80
0.90
1.00
-0.30
-0.20
-0.10
-0.00
0.10
0.20
0.30
X OVER DELTA
80°
70°
60°
50°
40°
30°
20°
10°
BETA =80.0 DEPTH =0.0870 FACTOR =0.0067

increasing with increasing phase angle. Their maxima are also separated, appearing to be on opposite sides of the conductor, which results in an interesting pattern for the ellipticity of the field ellipse. A good conductor changes the ellipse little, but a poor one varies it from near linear to a more circular polarization.

This was an effect observed in field tests (see Fig. 3) and hence not a result due only to the model. It is a consequence of the relative orientation of primary and secondary fields. As the primary major axis and secondary field vectors approach parallel orientation, the polarization tends towards linearity, but the ellipse becomes more circular, when summed near right angles.

To note the effects of depth on the computed anomalies, curves plotted in Figs. 20 to 23 were calculated. They represent depth variation for a fixed quality of conductor and a constant scale factor.

Dip angle curves tend to become broader with depth, while in-phase and quadrature maxima decrease in amplitude and increase in horizontal extent.

It was noted previously that conductor quality also had an effect on maximum amplitude (see Figs. 9 and 10), but in opposite fashions for the two axes. Increasing quality tends to increase in-phase response, but decrease quadrature response. Because the in-phase and quadrature values had been normalized for easy comparison with field values, it

Figs. 20, 21, 22, and 23. Depth variation for dip angle, field components and ellipticity at an ambient primary dip angle of 40°, a constant scale factor and a fixed quality of conductor (20°), based on Anderson and Sutherland's strong conductor.

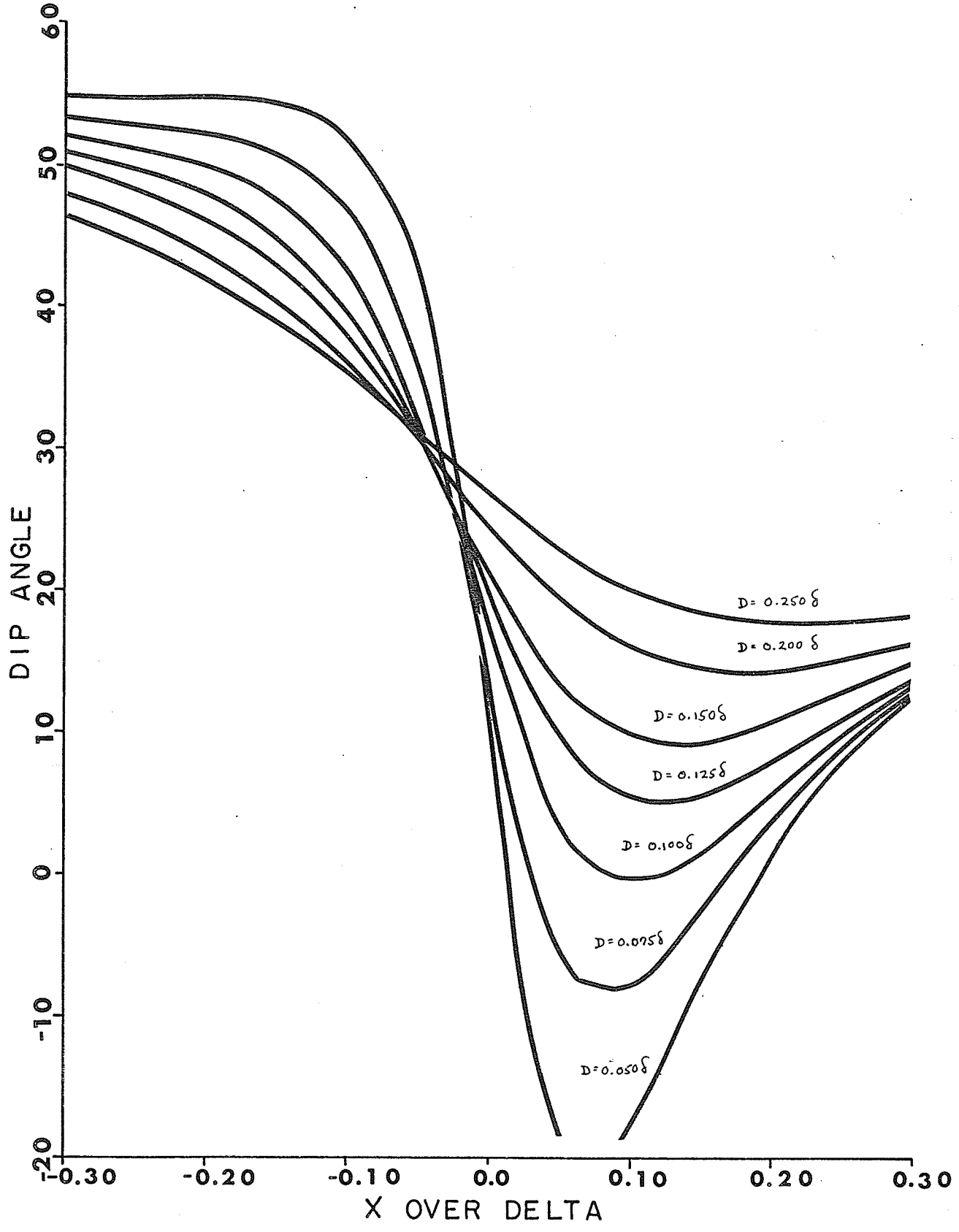
DIP ANGLE
60
50
40
30
20
10
0
-10
-20
-0.30
-0.20
-0.10
0.0
0.10
0.20
0.30
X OVER DELTA
D= 0.250 δ
D= 0.200 δ
D= 0.150δ
D= 0.125δ
D= 0.100δ
D= 0.075δ
D= 0.050δ

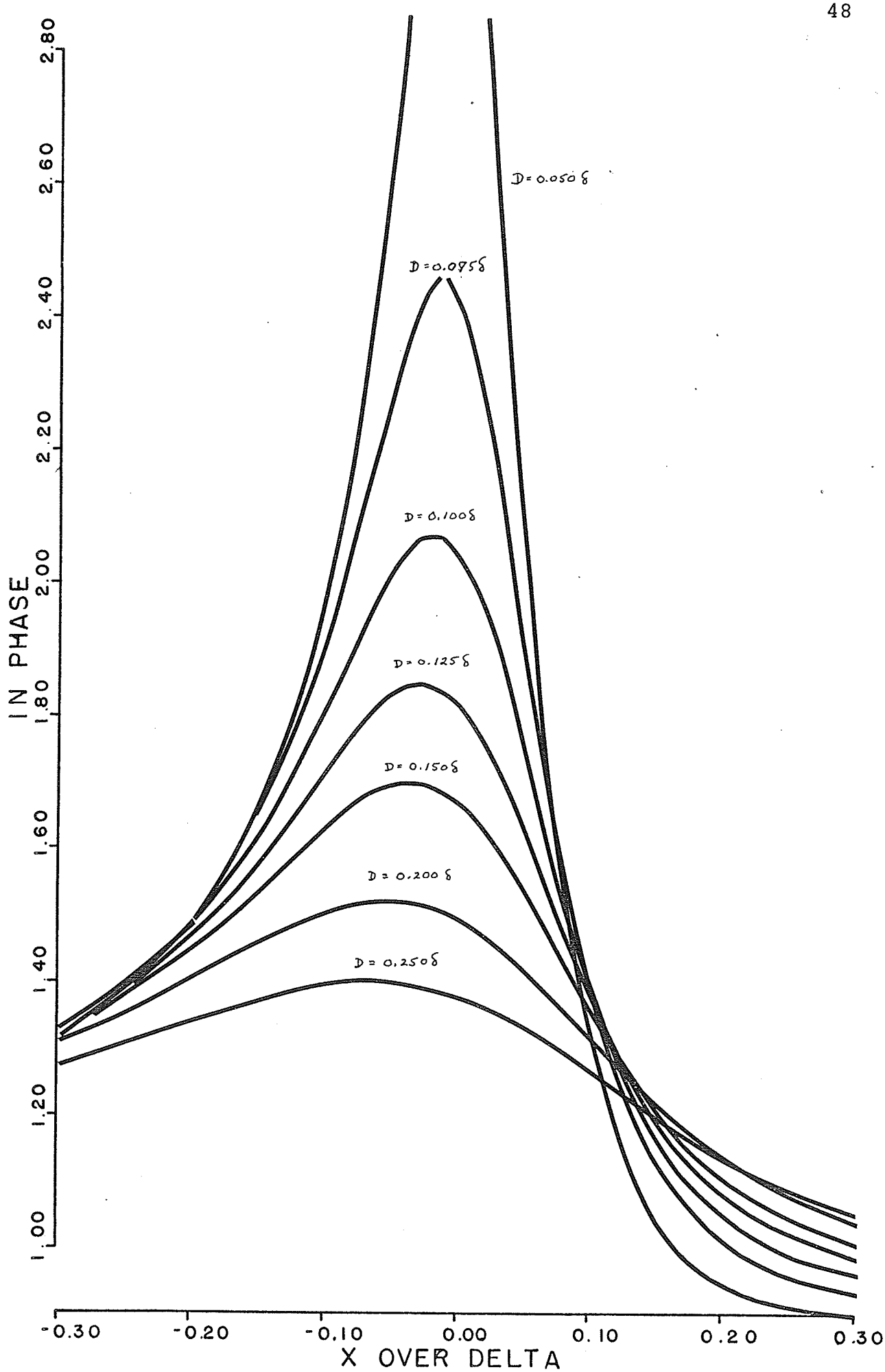
D = 0.050 δ
D = 0.075 δ
D = 0.100 δ
D = 0.125 δ
D = 0.150 δ
D = 0.200 δ
D = 0.250 δ
IN PHASE
2.80
2.60
2.40
2.20
2.00
1.80
1.60
1.40
1.20
1.00
-0.30
-0.20
-0.10
0.00
0.10
0.20
0.30
X OVER DELTA

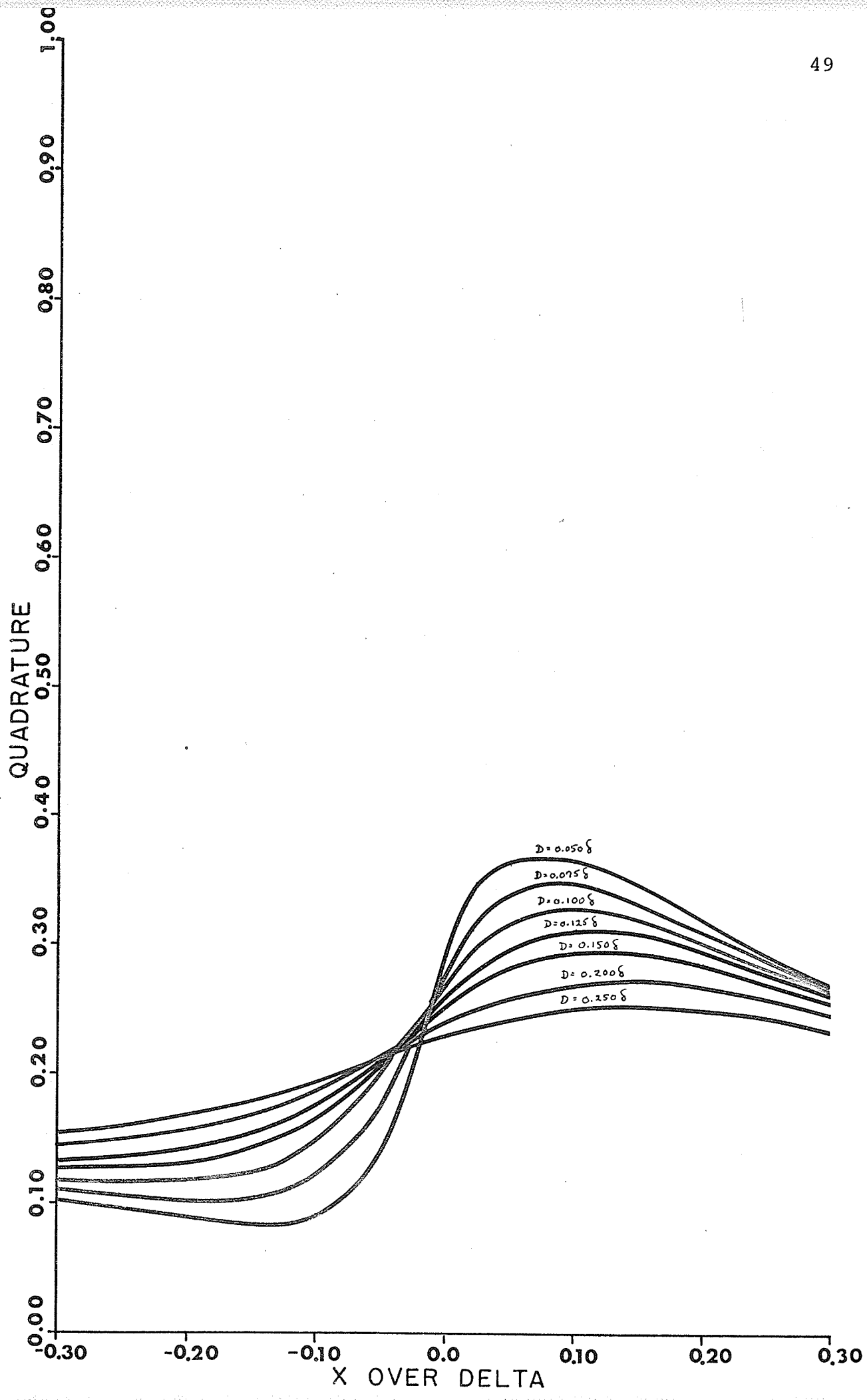
QUADRATURE
1.00
0.90
0.80
0.70
0.60
0.50
0.40
0.30
0.20
0.10
0.00
D = 0.050 δ
D = 0.075 δ
D = 0.100 δ
D = 0.125 δ
D = 0.150 δ
D = 0.200 δ
D = 0.250 δ
-0.30
-0.20
-0.10
0.0
0.10
0.20
0.30
X OVER DELTA

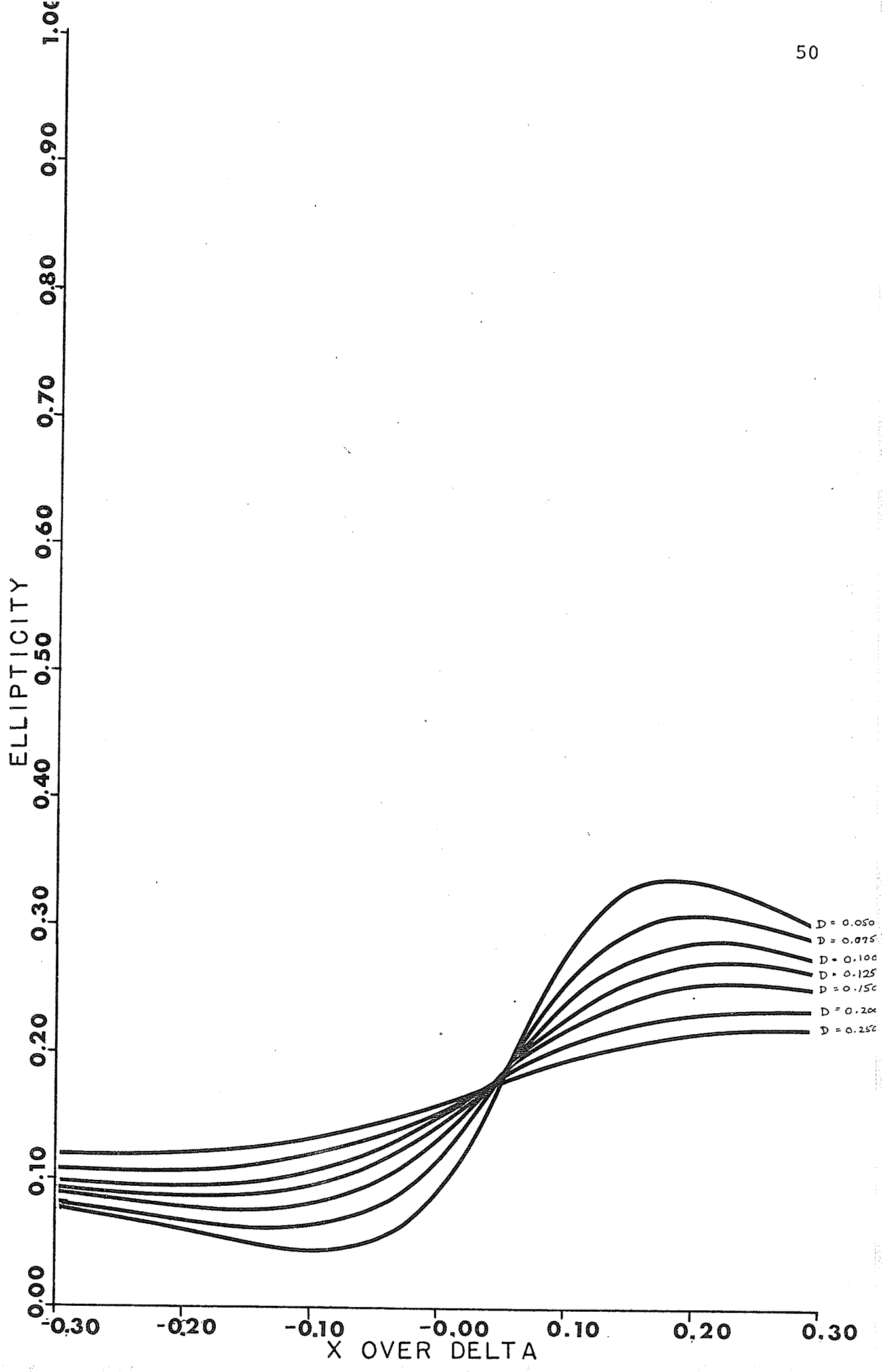
ELLIPTICITY
1.00
0.90
0.80
0.70
0.60
0.50
0.40
0.30
0.20
0.10
0.00
-0.30
-0.20
-0.10
-0.00
0.10
0.20
0.30
X OVER DELTA
D = 0.050
D = 0.075
D = 0.100
D = 0.125
D = 0.150
D = 0.200
D = 0.250

was thought that their maxima might be useful for an interpretation scheme. Plots of in-phase and quadrature maxima were made and Figs. 24 to 26 are the result.

Characterizing these are nearly horizontal lines of constant depth, especially for shallow bodies, and vertical to sloping lines of uniform quality. This would indicate that the normalized in-phase was more a measure of depth while normalized quadrature was a measure of quality. However, the scales chosen tend to accentuate the horizontal nature of the depth lines. In addition, no consideration was made for a change in current strength with conductor quality. A poor conductor has eddy currents of lesser amplitude (see Lamontagne and West, 1970), so that for this model, a poorer conductor would have a smaller scale factor. Because of the lack of field data, no changes were made for this effect, consequently, Figs. 24 to 26 are in error for poorer quality conductors. The lines of constant depth should be expected to lose their horizontal nature for decreasing quality of conductor.

Other data computed by the program included maximum and minimum dip angle slopes and their positions, as well as half maximum slope positions about the inflexion point, or point of minimum slope.

It was interesting to note that this model predicted a shift in the position of the inflexion point for increasing depth of conductor. As the depth increased, its position

Figs. 24, 25, and 26. Proposed graphs for the interpretation of DPM-2 field data using plots of the maximum in-phase and quadrature values over a responding body, divided by the in-phase value due to the primary field. Resulting depths are in terms of skin depth, and quality for the ribbon model, is listed as a phase angle from 5^{o} to 80^{o}. The figures are for fip angles of 40^{o}, 60^{o}, and 80^{o} respectively.

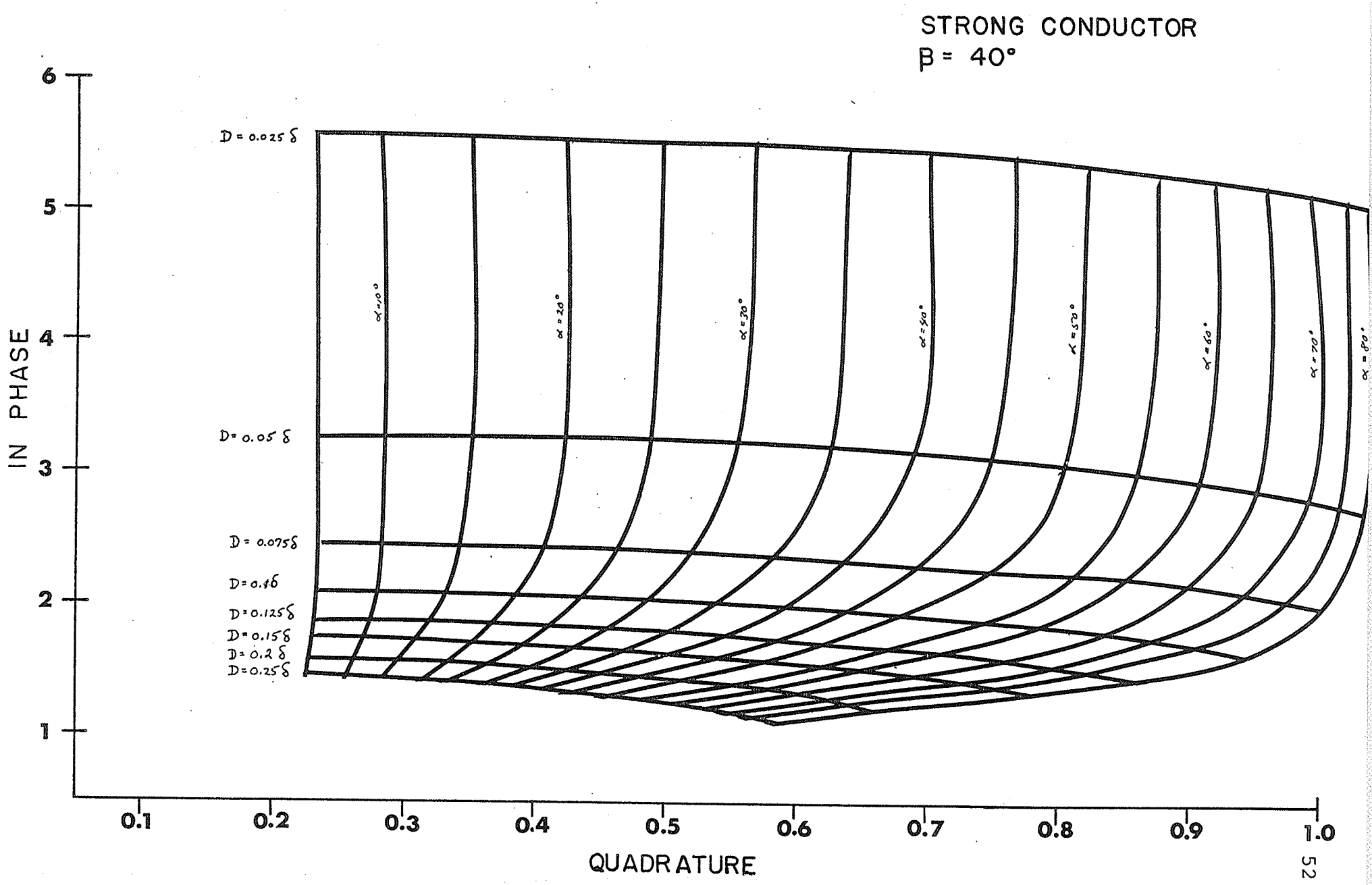
STRONG CONDUCTOR
β = 40°
IN PHASE
QUADRATURE
D = 0.025 δ
D = 0.05 δ
D = 0.075 δ
D = 0.1 δ
D = 0.125 δ
D = 0.15 δ
D = 0.2 δ
D = 0.25 δ
α = 10°
α = 20°
α = 30°
α = 50°
α = 70°
α = 80°
1
2
3
4
5
6
0.1
0.2
0.3
0.4
0.5
0.6
0.7
0.8
0.9
1.0

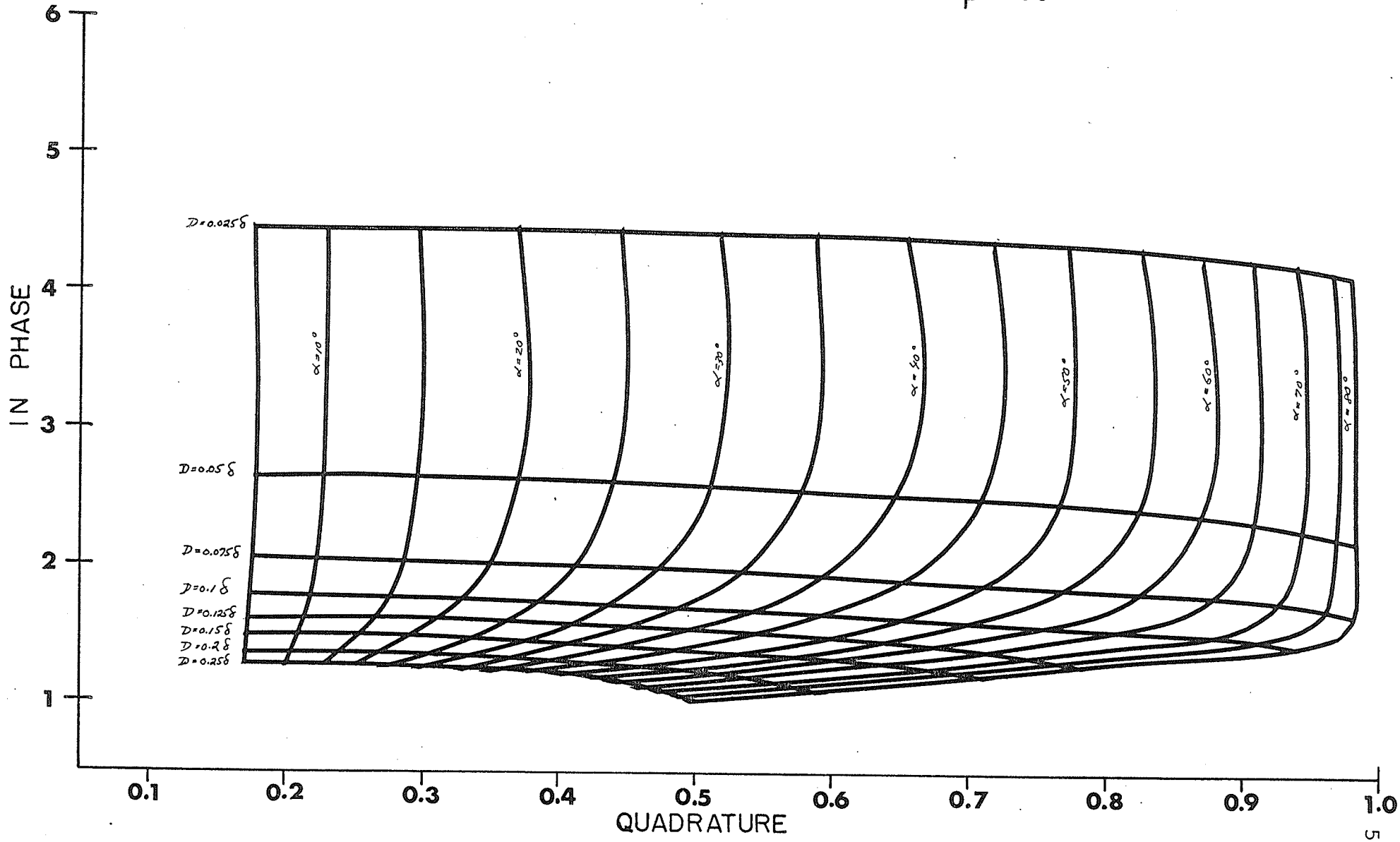
STRONG CONDUCTOR
β = 60°
IN PHASE
QUADRATURE
6
5
4
3
2
1
0.1
0.2
0.3
0.4
0.5
0.6
0.7
0.8
0.9
1.0
D=0.025δ
D=0.05δ
D=0.075δ
D=0.1δ
D=0.125δ
D=0.15δ
D=0.2δ
D=0.25δ
α=10°
α=20°
α=30°
α=40°
α=50°
α=60°
α=70°
α=80°

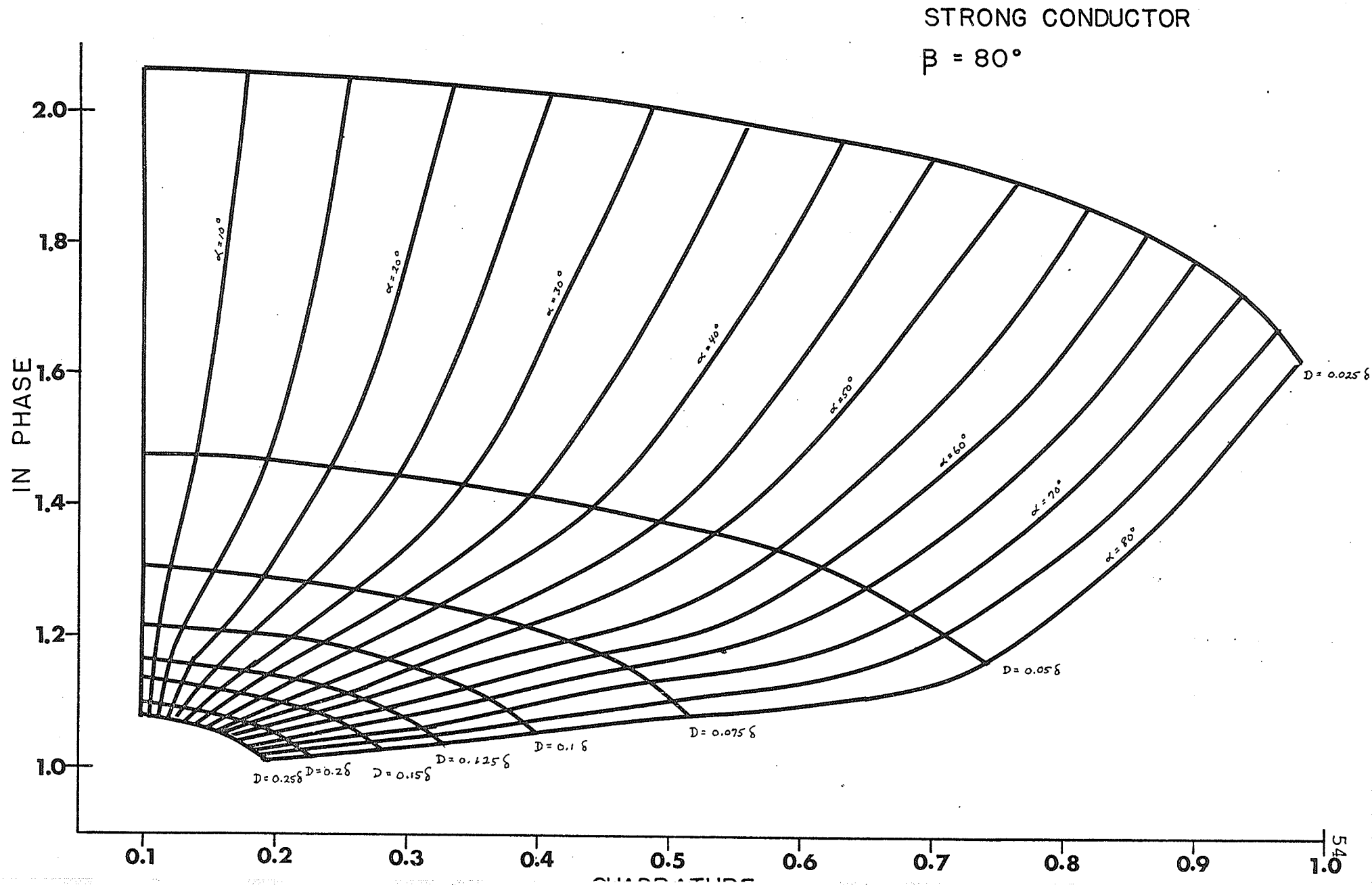
STRONG CONDUCTOR
β = 80°
IN PHASE
2.0
1.8
1.6
1.4
1.2
1.0
α=10°
α=20°
α=30°
α=40°
α=50°
α=60°
α=70°
α=80°
D= 0.025 δ
D= 0.05 δ
D= 0.075 δ
D= 0.1 δ
D= 0.125 δ
D= 0.15 δ
D= 0.2 δ
D= 0.25 δ
0.1
0.2
0.3
0.4
0.5
0.6
0.7
0.8
0.9
1.0

shifted towards the source cable. Table II illustrates this for three different quality conductors at dip angles of 40^{o}, 60^{o}, and 80^{o}. At 60^{o}, the maximum depth at which the inflexion point was still situated at the conductor axis was 0.075δ, 0.025δ less than the value at 40^{o}. At 80^{o}, the depth had decreased to 0.05δ.

For locating the conductor axis, no parameter other than the inflexion point seemed useful. Thus to locate axial position an accurate tabulation of inflexion point position with depth may be required. Future lab scale model studies should clarify this.

Table III lists half maximum slope positions and their differences in position for three different quality conductors at ambient dip angles of 40^{o}, 60^{o}, and 80^{o}. At these dip angles, there is little change in position with quality and the differences in position reflect a linear relationship with depth, for shallow depths.

Noting from Table II that slope position differences appeared to vary with quality as well as depth, suggested that plots of these differences versus half maximum slope position differences might be useful for a depth-quality interpretation scheme. However, the resulting plots (for example, see Fig. 27) do not give good definition of quality. Nevertheless, for DPM-1 data, this form of graph may be useful for estimating the depths of conductors.

Table II

Slope Positions

Phase	40° Dip Angle Slope Positions			60° Dip Angle Slope Positions			80° Dip Angle Slope Positions			Depth
	Min.	Max.	Diff.	Min.	Max.	Diff.	Min.	Max.	Diff.	
25°	-.005	.125	.13	-.005	.115	.12	-.005	.035	.04	.025
	-.005	.145	.15	-.005	.115	.12	-.015	.045	.06	.050
	-.005	.165	.17	-.005	.125	.13	-.025	.065	.09	.075
	-.005	.185	.19	-.015	.145	.16	-.035	.085	.12	.100
	-.015	.205	.22	-.025	.165	.19	-.055	.095	.15	.125
	-.015	.225	.24	-.035	.175	.21	-.065	.115	.18	.150
	-.035	.275	.31	-.045	.215	.26	-.095	.115	.21	.200
	-.045	.295	.34	-.065	.265	.33	-.125	.115	.24	.250
45°	-.005	.135	.14	-.005	.065	.07	-.005	.035	.04	.025
	-.005	.145	.15	-.005	.115	.12	-.015	.035	.05	.050
	-.005	.155	.16	-.005	.115	.12	-.035	.045	.08	.075
	-.005	.165	.17	-.015	.125	.14	-.045	.065	.11	.100
	-.015	.175	.19	-.025	.135	.17	-.055	.085	.14	.125
	-.015	.195	.21	-.035	.145	.18	-.075	.095	.17	.150
	-.035	.235	.27	-.055	.185	.24	-.105	.095	.20	.200
	-.045	.275	.32	-.075	.215	.29	-.135	.095	.23	.250
65°	-.005	.135	.13	-.005	.035	.03	-.005	.025	.02	.025
	-.005	.135	.13	-.005	.075	.07	-.015	.025	.04	.050
	-.005	.135	.14	-.005	.095	.10	-.035	.035	.07	.075
	-.005	.145	.15	-.015	.095	.11	-.055	.045	.10	.100
	-.015	.145	.16	-.025	.105	.13	-.075	.055	.13	.125
	-.025	.155	.18	-.045	.115	.16	-.085	.055	.14	.150
	-.035	.185	.22	-.065	.135	.20	-.125	.055	.18	.200
	-.055	.215	.27	-.095	.165	.26	-.165	.055	.22	.250

Table III

Half Maximum Slope Positions about the Point of Inflexion

Phase	40° Dip Angle Positions			60° Dip Angle Positions			80° Dip Amgle Positions			Depth
	Near	Far	Diff.	Near	Far	Diff.	Near	Far	Diff.	
25°	-.025	.025	.05	-.025	.025	.05	-.025	.015	.04	.025
	-.045	.035	.08	-.045	.035	.08	-.055	.005	.06	.050
	-.065	.045	.11	-.075	.035	.11	-.095	.005	.10	.075
	-.085	.055	.14	-.095	.045	.14	-.145	.005	.15	.100
	-.115	.055	.17	-.135	.045	.18	-.225	.015	.24	.125
	-.135	.065	.20	-.165	.045	.21	-.245	.015	NA	.150
	-.195	.085	.28	-.255	.055	.31	-.245	.035	NA	.200
	-.265	.105	.37	-.285	.065	.35	-.245	.075	NA	.250
45°	-.025	.025	.05	-.025	.025	.05	-.025	.015	.04	.025
	-.045	.035	.08	-.045	.035	.08	-.055	.005	.06	.050
	-.065	.045	.11	-.075	.035	.11	-.105	.005	.11	.075
	-.085	.055	.14	-.095	.035	.13	-.155	.005	.16	.100
	-.115	.055	.17	-.135	.035	.17	-.245	.005	NA	.125
	-.135	.065	.20	-.165	.035	.20	-.245	.005	NA	.150
	-.205	.085	.29	-.265	.045	.31	-.245	.035	NA	.200
	-.275	.105	.38	-.285	.055	.34	-.245	.075	NA	.250
65°	-.025	.025	.05	-.025	.025	.05	-.025	.005	.03	.025
	-.045	.035	.08	-.045	.055	.10	-.065	.005	.06	.050
	-.055	.035	.09	-.065	.045	.11	-.115	.005	.11	.075
	-.085	.045	.13	-.095	.035	.13	-.185	.015	.17	.100
	-.105	.055	.16	-.125	.025	.15	-.245	.005	NA	.125
	-.135	.065	.20	-.175	.025	.20	-.245	.005	NA	.150
	-.215	.095	.31	-.285	.015	.30	-.245	.025	NA	.200
	-.295	.115	.41	-.285	.025	.31	-.245	.155	NA	.250

Fig. 27. A possible interpretation scheme based on the differences in position of halfslopes, and the differences in position of maximum and minimum slope positions. Definition of quality is not as apparent here as in the proposed DPM-2 interpretation scheme.

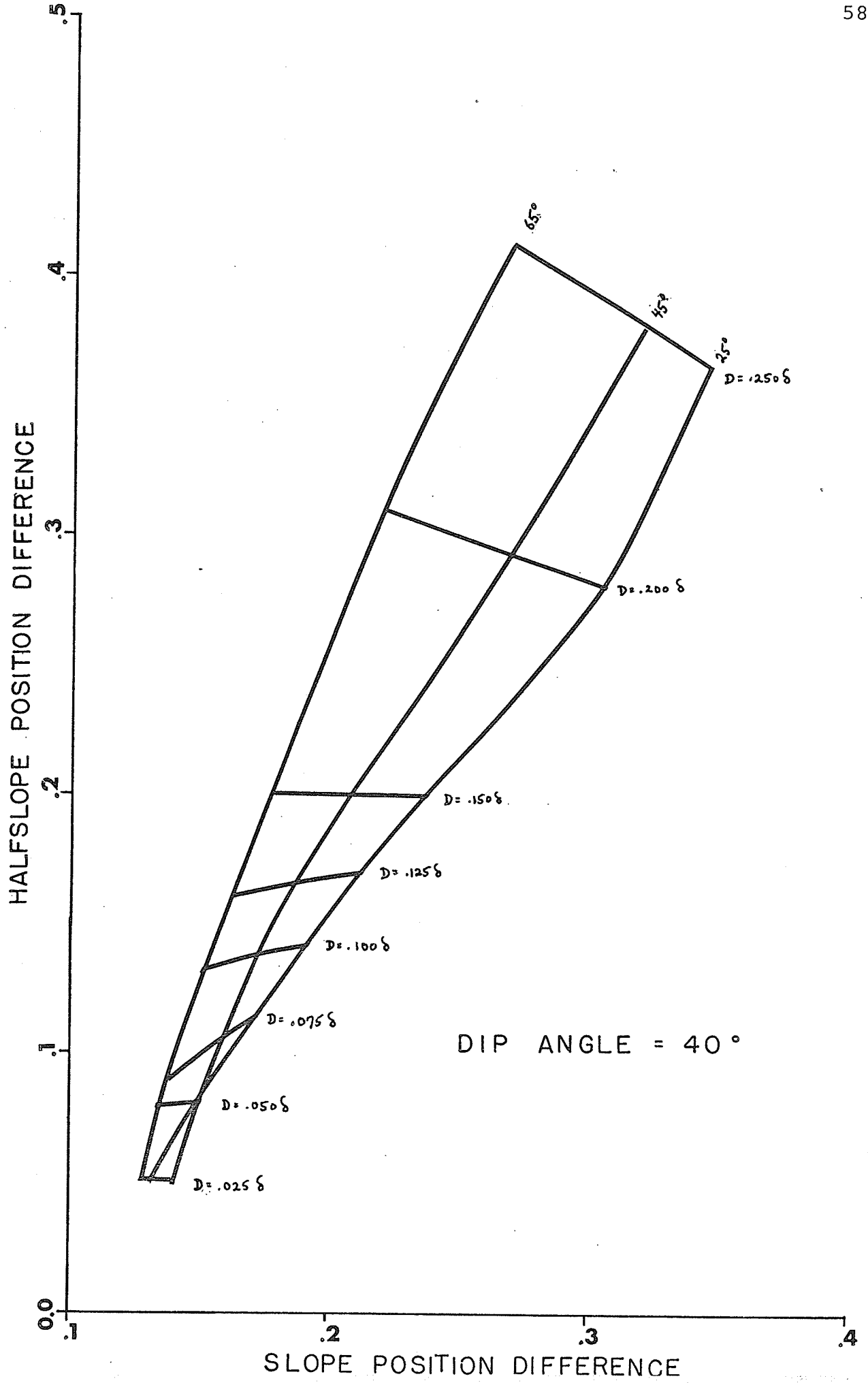
HALFSLOPE POSITION DIFFERENCE
SLOPE POSITION DIFFERENCE
0.0
.1
.2
.3
.4
.5
65°
45°
25°
D= .250 δ
D= .200 δ
D= .150 δ
D= .125 δ
D= .100 δ
D= .075 δ
D= .050 δ
D= .025 δ
DIP ANGLE = 40°

CHAPTER VIII

CONCLUSIONS

For the simple model employed, and the assumptions made for its use, the following conclusions may be drawn.

1. The similarity of computed anomalies and field curves suggest that the ribbon-current uniform field model is not unreasonable as an approximation.
2. Plots of half maximum slope position differences versus slope position differences do not give good detail for quality estimates, but depth estimates from DPM-1 data are possible.
3. In-phase and quadrature maxima appear to be the best measurements for use in an interpretation scheme which reveals both depth and quality.
4. The position of the point of inflexion is over the conductor for shallow depths, but shifts towards the source cable for greater depths. With variation in the ambient field dip angle, the maximum depth at which the inflexion point is still situated over the conductor axis varies. As the dip angle increases, this depth decreases.
5. Half maximum slope positions about the point of maximum inflexion appear to change little with

conductor quality. Position differences appear to vary linearly with depth for shallow depths.

LIST OF REFERENCES

Anderson, C.D. and D.B. Sutherland
1970 DPM-1: A long-wire dip angle electromagnetic method, a paper presented at the 40th Annual Meeting of the Society of Exploration Geophysicists, 1970.

Bezvoda, V.
1970 Fixed source system in a conductive environment, Geophysical Prospecting, vol. 18, No. 1, p. 47.

———— and K. Segeth
1970 A two layer ground in the field of an infinitely long cable, Geophysical Prospecting, vol. 18, No. 3, p. 343.

Bosschart, R.A.
1964 Analytic interpretation of fixed source electromagnetic prospecting data, Thesis, Uitgeverij Waltman-Delft, 102 pp.

Bursian, V.R.
1934 A normal field of an infinitely long straight cable (original in Russian), LGU Publisher, Leningrad.

Dizioglu, M.Y.
1967 Response of a two layer ground to an infinite cable carrying alternating current with reference to Turam Anomalies, Geophysical Prospecting, vol. 15, No. 3, p. 438.

Grant, F.S. and G.F. West
1965 Interpretation theory in applied geophysics, McGraw-Hill, Toronto, 584 pp.

Hohman, G.W.
1970 Electromagnetic scattering by two-dimensional inhomogeneities in the earth, Ph.D. Thesis, University of California, Berkeley.

Keller, G.V. and F.C. Frischkrecht
1966 Electrical methods in geophysical prospecting, Pergammon Press, Oxford.

Lamontagne, Y. and G.F. West
1970 Electromagnetic response of a rectangular thin plate, A paper presented at the 40th Annual Meeting of the Society of Exploration Geophysicists, 1970.

Paál, G.
1965 Ore prospecting based on VLF-radio signals, Geoexploration, vol. 3, No. 3, p. 139.

_____
1968 Very low frequency measurements made in Northern Sweden, Geoexploration, vol. 6, No. 3, p. 141.

Parasnis, D.S.
1966 Electromagnetic prospecting, Geoexploration, vol. 4, No. 4, p. 177.

Petrák, P.
1967 A normal field of an infinitely long cable according to the TURAM method (original in Czech) Journal Geologický průzkum, N° 11, Praha.

Ryu, J., H.F. Morrison and S.H. Ward
1970 Electromagnetic fields about a loop source of current, Geophysics, vol. 35, No. 5, p. 862.

Sundberg, K.
1931 Principles of the Swedish Geo-electrical methods, Erganzungshäfte für Angewandte Geophysik, vol. 1.

Ward, S.H.
1967 The electromagnetic method, in Mining Geophysics, vol. 2, p. 224.

West, G.F.
1960 Quantitative interpretation of electromagnetic induction measurements, Ph.D. Thesis, University of Toronto.

APPENDIX I

FORTRAN IV PROGRAM

A. Identification

1. Title — Calculation of the response over a line source
2. Programmer — D. Provins
3. Date — March, 1971

B. Purpose — To calculate the dip angle, in-phase, quadrature, and ellipticity over a line current.

C. Usage

1. Procedure — The main program calculates the expected response and plots the curves. Subroutine Plotter plots axes and parametric identification.
2. Parameters — Provided on a data card as follows:

columns 1-5: Primary field dip angle at the conductor's location.

columns 6-10: Depth to conductor in units of skin depth.

columns 11-15: Phase angle at which calculation is to commence.

columns 16-20: Scale factor.

columns 21-25: Survey line length, maximum of 6 units of

skin depth.

column 26: Set to 1 if all computed values are to be listed (default: no print-out).

column 27: Number of data cards.

column 28: Set to 1 to examine only the input phase angle (default is every value up to 90, in increments of 5 or 10).

column 29: Set of 1 to plot the data.

column 30: Set to 0, 1, 2, 3, or 4 for a survey line of 6, 3, 1.2, 0.6 or 0.3 when the input line length is 6 units.

column 31: Set of 1 to fix the dip angle at the value read in (default is variation according to position on the survey line).

column 32: Set to 1 to increment phase by 5 (default is 10).

column 33: Set to 1 to scale in-phase values by ½ (default is automatic scaling by ½ if a plotted value will exceed a 10 inch axis).

3. Space Requirements: 104k.

4. Print-out: Partly optional (col. 26). Characteristics of the responses are always listed.

5. Format: 5F5.2, 8I1

6. Time: Less than 30 sec. for plotting with a 5 increment from 0 to 90 phase.

7. Tapes: Plottape if plotting is desired.

8. Special JCL:

```
/*TAPE      PLOTTAPE                                    ..1
//GO. PLOTTAPE DD DSNAME = PLOT,
DISP .= SHR                                            ..2
```

if plotting is desired. For no plotting, remove card 1, and replace card 2 with: //GO. PLOTTAPE DD DUMMY

```
C
C     BETA IS AVERAGE PRIMARY FIELD DIP ANGLE AT THE CONDUCTOR POSITION
C
C     DEPTH IS CONDUCTOR DEPTH IN UNITS OF DELTA
C
C     ALPHA IS PHASE ANGLE BETWEEN PRIMARY AND SECONDARY FIELD
C
C     FACTOR IS THE SCALE FACTOR
C
C     LINE IS THE SURVEY LINE LENGTH,& MAY NOT EXCEED 6 UNITS
C
C     IF IPRINT EQUALS 1,DATA VALUES ARE PRINTED OUT, OTHERWISE,
C     IPRINT SHOULD BE ZERO.
C
C     M IS THE NUMBER OF DIFFERENT  PLOTS
C
C     IF I1 IS 1, ONLY ONE VALUE OF PHASE IS EXAMINED
C
C     IF I2 IS 1, THE DATA IS PLOTTED FOR A MULTIPLE OF 6 LINE UNITS
C
C     FOR I3=0,1,2,3,OR4, LINE IS 6,3,1.2,.6,OR .3 UNITS LONG
C     RESPECTIVELY, FOR A LINE VALUE OF 6 UNITS
C
C     IF I4 IS 0, THE DIP ANGLE CHANGES WITH POSITION
C
C     IF I5 IS 1, PHASE IS INCREMENTED BY 5 DEGREES, DEFAULT IS 10 DEGREES
C
C     IF I6 IS 1, PLOTTED IN PHASE VALUES ARE SCALED BY 1/2.
C
      DIMENSION IBUF(4000),X(1200),IN(1200),OUT(1200),ELLIP(1200),ANGL(1
     1200)
      INTEGER T
      REAL OMGAT1,OMGAT2,INP,OUTR,IN,OUT,LINE
      DATA 00,01,02,03,04,05/-0.11823542E-3,-0.18065605E-4,
     10.32466973E-3,-0.75471628E-5,0.51110070E-7,-0.81660166E-10/
C
C     READ IN INPUT PARAMETERS FOR FIRST AND SUBSEQUENT RUNS.
C
      READ (5,1) BETA,DEPTH,ALPHA,FACTOR,LINE,IPRINT,M,I1,I2,I3,I4,I5,I6
1     FORMAT (5F5.2,8I1)
      T=M
      N=1
C
C     SET UP FOR PLOTTING DEVICE
C
      CALL PLOTS (IBUF,4000)
50    WRITE (6,200) BETA
200   FORMAT (1H1,'BETA   EQUALS ',F10.5)
      WRITE (6,220) DEPTH
220   FORMAT (' ','DEPTH  EQUALS ',F10.5)
      WRITE (6,300) FACTOR
300   FORMAT (1H ,'FACTOR EQUALS ',F10.5)
      WRITE (6,40)
40    FORMAT (1H0)
C
C     PRINT OUT PARAMETERS IF DESIRED
C
      IF (IPRINT.EQ.0) GO TO 16
```

```
      WRITE (6,15)
15    FORMAT (4X,'XTRN',6X,'PHASE',7X,'IN',8X,'OUT',6X,'ANGLE',3X,'ELLIP
     1TICITY')
      WRITE (6,40)
C
C     SET UP INITIAL PARAMETERS
C
16    CONTINUE
      J=1
      ZMAX=0.
      ZMIN=999.
      BETI=BETA
      IF (I4.NE.0) BETI=BETT
      IF (BETI.LE.1.) BET1=BETI
      IF (BETI.LE.1.) GO TO 91
      XOD=2.1757132*ALOG(90./BETI)
91    BETA=BETA*3.14159/180.
      IF (LINE.GT.6.) LINE=6.
      IF (I2.EQ.1) LINE=6.
17    CONTINUE
      PHAS=ALPHA
      ALPHA=ALPHA*3.14159/180.
      XTRN=-LINE/2.
      IF (I3.EQ.1) XTRN=XTRN/2.
      IF (I3.EQ.2) XTRN=XTRN/5.
      IF (I3.EQ.3) XTRN=XTRN/10.
      IF (I3.EQ.4) XTRN=XTRN/20.
      REF=XTRN
      SLOP=0.
      HAFMN1=999.
      HAFMN2=999.
      OUTMAX=0.
      OUTMIN=999.
      ZMAX=0.
      ANG=-999.
      AMAX=0.
      AMIN=999.
      K=1
      SLMAX=1.E-3
      SLMIN=999.
      SLOP2=0.
      EMAX=0.
      EMIN=999.
C
C     CALCULATE DIP ANGLE, IN AND OUT OF PHASE, AND ELLIPTICITY FOR
C     VARIOUS PHASE ANGLES
C
2     CONTINUE
      THETA=ATAN(XTRN/DEPTH)
      X(J)=XTRN
      IF (BETI.LE.1.) GO TO 92
      IF (I4.EQ.0) BETA=3.14159/2.*EXP(-.4596194*(X(J)+XOD))
      IF (I4.EQ.0) BET1=90.*EXP(-.4596194*(X(J)+XOD))
92    R=FACTOR/SQRT(X(J)**2+DEPTH**2)
      C=Q0+Q1*BET1**1+Q2*BET1**2+Q3*BET1**3+Q4*BET1**4+Q5*BET1**5
      AI=COS(BETA)
      BI=COS(ALPHA)*COS(THETA)*R
      CI=SIN(ALPHA)*COS(THETA)*R+C*SIN(BETA)
```

```
      DI=SIN(THETA)*COS(ALPHA)*P
      BI=SIN(ALPHA)*SIN(THETA)*B+C*COS(BETA)
      FI=SIN(BETA)
      P=BI*(FI-DI)-CI*(BI+AI)
      Q=(AI+BI)**2-CI**2-FI**2+(DI-FI)**2
C
C     ROUTINE FOR ZERO DENOMINATOR
C
      S=ABS(P)
      IF (S.LT.1.E-8) OMGAT1=0.
      IF (S.LT.1.E-8) OMGAT2=3.14159/2.
      IF (S.LE.1.E-8) GO TO 188
C
C     CALCULATE X AND Y COMPONENTS
C
      ROOT=SQRT(Q*Q/P/P+4.)
      OMGAT1=ATAN((-Q/P+ROOT)/2.)
      OMGAT2=ATAN((-Q/P-ROOT)/2.)
188   RXSQT1=((AI+BI)*SIN(OMGAT1)+CI*COS(OMGAT1))**2
      RXSQT2=((AI+BI)*SIN(OMGAT2)+CI*COS(OMGAT2))**2
      RYSQT1=((DI-FI)*SIN(OMGAT1)+EI*COS(OMGAT1))**2
      RYSQT2=((DI-FI)*SIN(OMGAT2)+EI*COS(OMGAT2))**2
C
C     CALCULATE VECTOR MAGNITUDES
C
      RMAGT1=SQRT(RXSQT1+RYSQT1)
      RMAGT2=SQRT(RXSQT2+RYSQT2)
      IF (RMAGT1-RMAGT2) 199,199,400
C
C     ASSIGN IN AND OUT OF PHASE VALUES
C
199   INR=RMAGT2
      OUTR=RMAGT1
      DIRCOS=((AI+BI)*SIN(OMGAT2)+CI*COS(OMGAT2))/RMAGT2*(-1.)
      DIRSIN=((DI-FI)*SIN(OMGAT2)+EI*COS(OMGAT2))/RMAGT2
      IF (DIRCOS.GT.1.) DIRCOS=1.
      GO TO 600
C
C     ASSIGN IN AND OUT OF PHASE VALUES
C
400   INR=RMAGT1
      OUTR=RMAGT2
      DIRCOS=((AI+BI)*SIN(OMGAT1)+CI*COS(OMGAT1))/RMAGT1*(-1.)
      DIRSIN=((DI-FI)*SIN(OMGAT1)+EI*COS(OMGAT1))/RMAGT1
      IF (DIRCOS.GT.1.) DIRCOS=1.
C
C     CALCULATE DIP ANGLE
C
600   ANGLE=ARSIN(DIRSIN)
C
C     PUT DIP ANGLE IN PROPER QUADRANT
C
      IF (DIRCOS.LT.0..AND.DIRSIN.GT.0.) ANGLE=3.14159-ANGLE
      IF (DIRCOS.LT.0..AND.DIRSIN.LT.0.) ANGLE=ABS(ANGLE)
      ANGLE=ANGLE*180./3.14159
      IF (BETA.LT.60.0.AND.ANGLE.GT.90.0) ANGLE=ANGLE-180.0
      IF (ANGLE.GT.135.0) ANGLE=ANGLE-180.0
C
```

```
C       SCALE IN AND OUT OF PHASE, ELLIPTICITY, AND DIP ANGLE
C
        IF (I4.EQ.0.AND.BETI.GT.90.) INR=1.
        IF (I4.EQ.0.AND.BETI.GT.90.) OUTR=0.
        IF (I4.EQ.0.AND.BETI.GT.90.) ANGLE=0.
        IN(J)=INR*10.
        OUT(J)=OUTR*10.
        ELLIP(J)=OUTR/INR*10.
        ANGL(J)=(ANGLE-BETI+50.)/10.
        IF (I4.EQ.0.AND.BETI.GT.90.) ANG=(90.-BETI+50.)/10.
        IF (I4.EQ.0.AND.BETI.GT.90.) ANGL(J)=ANG
C
C       CALCULATE EXTREME VALUES OF IN AND OUT OF PHASE, AND ELLIPTICITY
C
        IF (I4.EQ.0.AND.BETI.GT.90.) GO TO 419
        IF (INR.GE.ZMAX) ZMAX=INR
        IF (INR.GT.ZMAX) XI=X(J)
        IF (INR.GE.ZMAI) ZMAI=INR
        IF (INR.GE.ZMAI) XO=X(J)
        IF (INR.LE.ZMIN) ZMIN=INR
        IF (INR.LE.ZMIN) XMIN=X(J)
        IF (OUTR.GE.OUTMAX) OUTMAX=OUTR
        IF (OUTR.GE.OUTMAX) XO1=X(J)
        IF (OUTR.LE.OUTMIN) OUTMIN=OUTR
        IF (OUTR.LE.OUTMIN) XO2=X(J)
        IF (ELLIP(J).GE.EMAX) EMAX=ELLIP(J)
        IF (ELLIP(J).GE.EMAX) XO3=X(J)
        IF (ELLIP(J).LE.EMIN) EMIN=ELLIP(J)
        IF (ELLIP(J).LE.EMIN) XO4=X(J)
C
C       FIND THE MINIMUM ANGLE AND EXTREME VALUES OF SLOPE
C
        IF (ANGLE.GE.AMAX.AND.X(J).LT.0.) AMAX=ANGLE
        IF (ANGLE.GE.AMAX.AND.X(J).LT.0.) XANG1=X(J)
        IF (ANGLE.LE.AMIN) AMIN=ANGLE
        IF (ANGLE.LE.AMIN) XANG=X(J)
        IF (K.LE.2) GO TO 419
        IF (ABS(ANGL(J-2)-ANG).LT.1.E-3) GO TO 419
        SLOP2=ANGL(J)-ANGL(J-1)
        IF (SLOP2.LE.SLMIN.AND.X(J-2).LE.0.) SLMIN=SLOP2
        IF (SLOP2.GE.SLMAX) SLMAX=SLOP2
        IF (SLOP2.LE.SLMIN.AND.X(J-2).LE.0.) XSLMIN=(X(J)+X(J-1))/2.
        IF (SLOP2.GT.SLMAX) XSLMAX=(X(J)+X(J-1))/2.
419     CONTINUE
C
C       PRINT CALCULATED VALUES
C
        IF (IPRINT.EQ.0) GO TO 34
        ELLIPT=ELLIP(J)/10.
        WRITE (6,3) XTEN,PHAS,INR,OUTR,ANGLE,ELLIPT
3       FORMAT (6F10.4)
C
C       INCREMENT XTEN
C
34      XTEN=XTEN+0.10
        IF (I3.EQ.1) XTEN=(X(J)*2.0+0.10)/2.0
        IF (I3.EQ.2) XTEN=(X(J)*5.0+0.10)/5.0
        IF (I3.EQ.3) XTEN=(X(J)*10.+0.10)/10.
```

```
      IF (I3.EQ.4) XTRN=(X(J)*20.+0.10)/20.
      K=K+1
      J=J+1
      IF (I3.EQ.0.AND.XTRN.LE.(LINE/2.)) GO TO 2
      IF (I3.EQ.1.AND.XTRN.LE.(LINE/4.)) GO TO 2
      IF (I3.EQ.2.AND.XTRN.LE.(LINE/10.)) GO TO 2
      IF (I3.EQ.3.AND.XTRN.LE.(LINE/20.)) GO TO 2
      IF (I3.EQ.4.AND.XTRN.LE.(LINE/40.)) GO TO 2
C
C       INCREMENT PHASE ANGLE AND FIND HALFSLOPE POSITIONS ABOUT THE
C     POINT OF MAXIMUM INFLEXION
C
      HAFSLP=SLMIN/2.
      DO 999 L=3,K
      IF (L.EQ.M) GO TO 990
      SLOP=ANGL(L)-ANGL(L-1)
990   IF (X(L).LT.XSLMIN.AND.ABS(SLOP-HAFSLP).LE.HAFMN1) HAFMN1=ABS(SLOP
     1-HAFSLP)
      IF (X(L).LT.XSLMIN.AND.ABS(SLOP-HAFSLP).LE.HAFMN1) XHAF1=(X(L)+X(L
     1-1))/2.
      IF (X(L).GT.XSLMIN.AND.ABS(SLOP-HAFSLP).LE.HAFMN2.AND.X(L).LE.XANG
     1) HAFMN2=ABS(SLOP-HAFSLP)
      IF (X(L).GT.XSLMIN.AND.ABS(SLOP-HAFSLP).LE.HAFMN2.AND.X(L).LE.XANG
     1) XHAF2=(X(L)+X(L-1))/2.
999   CONTINUE
      EMAX=EMAX/10.
      EMIN=EMIN/10.
C
C     PRINT OUT THE MAXIMUM AND MINIMUM OF IN-PHASE, QUADRATURE AND
C     ELLIPTICITY, AND THEIR POSITIONS
C     PRINT OUT THE SLOPES,THEIR POSITIONS, AND THE HALFSLOPE POSITIONS.
C     PRINT OUT THE MAXIMUM AND MINIMUM DIP ANGLES AND THEIR POSITIONS.
C
      WRITE (6,70) PHAS,ZMAX,XI,OUTMAX,XD1,OUTMIN,XD2,EMIN,XD4,EMAX,XD3
70    FORMAT (1X,'PHASE',F4.1,' ZMAX',F10.5,' X',F7.3,' OMAX',F10.5,' X'
     1,F7.3,' OMIN',F10.5,' X',F7.3,' EMIN',F10.5,' X',F7.3,' EMAX',
     1F10.5,' X',F6.3)
      SLRAT=(-SLMIN)/SLMAX
      SLMIN=SLMIN*10./(X(J-1)-X(J-2))
      SLMAX=SLMAX*10./(X(J-1)-X(J-2))
      WRITE (6,998) SLMIN,XSLMIN,SLMAX,XSLMAX,SLRAT
998   FORMAT (1X,'SLMIN =',F12.2,' X =',F9.3,' SLMAX =',F12.2,' X =',F9.
     13,' SLRATIO =',F15.7)
      WRITE (6,997) XHAF1,XHAF2,AMIN,XANG,AMAX,XANG1
997   FORMAT (1X,'HALFSLOPE AT',F9.3,' AND',F9.3,'  MINIMUM DIP ANGLE OF
     1',F9.3,' AT',F9.3,' MAXIMUM DIP OF',F9.3,' AT',F9.3)
      WRITE (6,40)
      PINC=10.
      IF (I5.EQ.1) PINC=5.
      PHAS=PHAS+PINC
      ALPHA=PHAS
      IF (I1.EQ.1) ALPHA=85.
      IF (I1.NE.1) PHAS=PHAS-PINC
      IF (ALPHA.GT.90.0) J=J-1
      IF (ALPHA.GT.80.0) GO TO 101
      WRITE (6,5)
5     FORMAT (1H )
      GO TO 17
```

```
101   WRITE (6,68) OUTMAX,XD1,ZMAX,XMAX,BSTI,DEPTH,FACTOR
68    FORMAT (1X,'OUTMAX =',F10.5,' X =',F10.5,' IMAX =',F10.5,' X =',
     1F10.5,' BSTI =',F10.5,' DEPTH =',F10.5,' FACTOR =',F10.5)
      WRITE (6,69) OUTMIN,XD2,ZMIN,XMIN
69    FORMAT (' ','OUTMIN =',F10.5,2X,' X = ',F10.5,' IMIN =',F10.5,
     1' X =',F10.5)
      WRITE (6,405) N,T
405   FORMAT (10X,I5,'  OF',I3)
      IF (I2.EQ.0) GO TO 104
C
C     SET UP ORIGIN FOR DIP ANGLE PLOT
C
      CALL PLOT (0.,-2.,3)
      CALL PLOT (LINE,00.,-3)
      I7=1
C
C     PLOT DIP ANGLE
C
      FIRSTV=BSTI-60.0
      XPAGE=LINE/2.+.25
      XTEN=-LINE/2.
      CALL AXIS (XTEN,-1.,9HDIP ANGLE,9,8.,90.,FIRSTV,10.)
      CALL PLOTER (LINE,XPAGE,XTEN,BSTI,PHAS,I1,I7,DEPTH,I3,FACTOR)
      DO 28 L=1,J
      IF (I3.EQ.1) X(L)=X(L)*2.
      IF (I3.EQ.2) X(L)=X(L)*5.
      IF (I3.EQ.3) X(L)=X(L)*10.
      IF (I3.EQ.4) X(L)=X(L)*20.
28    CONTINUE
      DO 29 L=1,J
      IPEN=2
      IF (I4.EQ.0.AND.ANGL(L).EQ.ANG) IPEN=3
      IF (L.EQ.1) GO TO 801
      IF (I4.EQ.0.AND.ANGL(L-1).EQ.ANG) IPEN=3
801   CONTINUE
      IF (ABS(X(L)+LINE/2.).LT.1.E-3) IPEN=3
      IF (ANGL(L).LT.-.9) CALL SYMBOL (X(L),-.9,.14,6,180.,-1)
      IF (ANGL(L).LT.-.9) GO TO 29
      IF (ANGL(L).GT.8.4) CALL SYMBOL (X(L),8.5,.14,6,0.,-1)
      IF (ANGL(L).GT.8.4) GO TO 29
      CALL PLOT (X(L),ANGL(L),IPEN)
29    CONTINUE
C
C     PLOT OUT OF PHASE
C
113   CALL PLOT (0.,-1.50,-3)
      I7=0
      CALL PLOT (8.5,0.,-3)
      XTEN=-LINE/2.
      CALL AXIS (XTEN,0.,10HQUADRATURE,10,10.,90.,0.,.1)
      CALL PLOTER (LINE,XPAGE,XTEN,BSTI,PHAS,I1,I7,DEPTH,I3,FACTOR)
      DO 105 L=1,J
      IPEN=2
      IF (I4.EQ.0.AND.ANGL(L).EQ.ANG) IPEN=3
      IF (L.EQ.1) GO TO 802
      IF (I4.EQ.0.AND.ANGL(L-1).EQ.ANG) IPEN=3
802   CONTINUE
      IF (ABS(X(L)+LINE/2.).LT.1.E-3) IPEN=3
```

```
      IF (OUT(L).GT.10.) IPEN=3
      IF (OUT(L).GT.10.) OUT(L)=10.01
      IF (L.EQ.1) GO TO 114
      IF (OUT(L-1).GT.10.) IPEN=3
114   CONTINUE
      CALL PLOT (X(L),OUT(L),IPEN)
105   CONTINUE
      CALL PLOT (8.5,0.,-3)
C
C     PLOT ELLIPTICITY
C
      CALL AXIS (XTEN,0.,11HELLIPTICITY,11,10.,90.,0.,.1)
      CALL PLOTER (LINE,XPAGE,XTEN,BETI,PHAS,I1,I7,DEPTH,I3,FACTOR)
      DO 111 L=1,J
      IPEN=2
      IF (I4.EQ.0.AND.ANGL(L).EQ.ANG) IPEN=3
      IF (L.EQ.1) GO TO 803
      IF (I4.EQ.0.AND.ANGL(L-1).EQ.ANG) IPEN=3
803   CONTINUE
      IF (ABS(X(L)+LINE/2.).LT.1.E-3) IPEN=3
      IF (OUT(L).GT.10.) IPEN=3
      IF (L.EQ.1) GO TO 115
      IF (OUT(L-1).GT.10.) IPEN=3
115   CONTINUE
      CALL PLOT (X(L),ELLIP(L),IPEN)
111   CONTINUE
      CALL PLOT (8.5,0.,-3)
C
C     PLOT IN PHASE
C
      IF (I6.EQ.1) GO TO 504
      II=0
      DO 503 L=2,J
      IF (ANGL(L-1).EQ.ANG) GO TO 503
      IF (ABS(IN(L)-ZMIN*10.).GT.10.) II=1
      IF (II.EQ.1) L=J
503   CONTINUE
      IF (II) 506,506,504
504   DO 506 L=1,J
      IN(L)=IN(L)/2.
506   CONTINUE
      YINC=0.1
      IF (I6.EQ.1) YINC=0.2
      IF (II.EQ.1) YINC=0.2
      INT=ZMIN*10.
      FIRSTV=INT+1
      YPAGE=FIRSTV-ZMIN*10.
      FIRSTV=FIRSTV/10.
      IF (II.EQ.1.OR.I6.EQ.1) YPAGE=YPAGE/2.
      CALL AXIS (XTEN,YPAGE,8HIN PHASE,8,9.,90.,FIRSTV,YINC)
      CALL PLOTER (LINE,XPAGE,XTEN,BETI,PHAS,I1,I7,DEPTH,I3,FACTOR)
      IF (II.EQ.1.OR.I6.EQ.1) ZMIN=ZMIN/2.
      DO 103 L=1,J
      IN(L)=IN(L)-ZMIN*10.
      IPEN=2
      IF (I4.EQ.0.AND.ANGL(L).EQ.ANG) IPEN=3
      IF (L.EQ.1) GO TO 804
      IF (I4.EQ.0.AND.ANGL(L-1).EQ.ANG) IPEN=3
```

```
804   CONTINUE
      IF (ABS(X(L)+LINE/2.).LT.1.E-3) IPEN=3
      IF (IN(L).GT.10.) IN(L)=10.1
      IF (IN(L).GT.10.) IPEN=3
      CALL PLOT (X(L),IN(L),IPEN)
103   CONTINUE
      CALL PLOT (2.5,0.,-3)
104   CONTINUE
      M=N+1
C
C
C       READ THE NEXT DATA CARD, IF ANY.
      IF (N.LE.T) READ (5,1) BETA,DEPTH,ALPHA,FACTOR,LINE,IPRINT,M,I1,I2
     1,I3,I4,I5,I6
      IF (N.LE.T) GO TO 53
C
C       CLOSE THE PLOT DEVICE AND END EXECUTION.
C
      CALL PLOT (0.,0.,999)
      CALL EXIT
      END
```

```
      SUBROUTINE PLOTSB (LINE,XPAGE,XTRN,BETT,PHAS,I1,I7,DEPTH,I3,FACTOR
     1)
      Y=0.
      IF (I7.EQ.1) Y=-1.
      FIRST=XTRN
      D=1.
      IF (I3.EQ.1) FIRST=XTRN/2.
      IF (I3.EQ.2) FIRST=XTRN/5.
      IF (I3.EQ.3) FIRST=XTRN/10.
      IF (I3.EQ.4) FIRST=XTRN/20.
      IF (I3.EQ.1) D=0.5
      IF (I3.EQ.2) D=0.2
      IF (I3.EQ.3) D=0.1
      IF (I3.EQ.4) D=0.05
      CALL AXIS (XTRN,Y,12HX OVER DELTA,-12,LINE,0.,FIRST,D)
      CALL SYMBOL (XPAGE,1.,.14,6HBETA =,90.,6)
      CALL NUMBER (XPAGE,999.,.14,BETT,90.,1)
      CALL SYMBOL (XPAGE,2.5,.14,7HDEPTH =,90.,7)
      CALL NUMBER (XPAGE,999.,.14,DEPTH,90.,4)
      CALL SYMBOL (XPAGE,4.5,.14,8HFACTOR =,90.,8)
      CALL NUMBER (XPAGE,999.,.14,FACTOR,90.,4)
      IF (I1.EQ.1) CALL SYMBOL (XPAGE,6.5,.14,7HPHASE =,90.,7)
      IF (I1.EQ.1) CALL NUMBER (XPAGE,999.,.14,PHAS,90.,1)
      RETURN
      END
```

SUBPROGRAMS CALLED

LOCATION	SYMBOL	LOCATION	SYMBOL	LOCATION	SYMBOL	LOCATIO
360	PLOTS	364	PLOT	368	AXIS	36C
374	EXIT	378	ALOG	37C	ATAN	380
388	COS	38C	SIN	390	ARSIN	394

SCALAR MAP

LOCATION	SYMBOL	LOCATION	SYMBOL	LOCATION	SYMBOL	LOCATIO
654	Q1	658	Q2	65C	Q3	660
669	BETA	66C	DEPTH	670	ALPHA	674
67C	IPRINT	680	M	684	I1	688
690	I4	694	I5	698	I6	69C
6A4	J	6A8	ZMA1	6AC	ZMIN	6B0
6B8	XOD	6BC	PHAS	6C0	XTEN	6C4
6CC	HAFMN1	6D0	HAFMN2	6D4	OUTMAX	6D8
6E0	ANG	6E4	AMAX	6E8	AMIN	6EC
6F4	SLMIN	6F8	SLOP2	6FC	RMAX	700
708	B	70C	C	710	AI	714
71C	DT	720	EI	724	FI	728
730	S	734	OMGAT1	738	OMGAT2	73C
744	RXSQT2	748	RYSQT1	74C	RYSQT2	750
758	INR	75C	CUTR	760	DIRCOS	764
76C	XI	770	XD	774	XMIN	778
780	XD3	784	XD4	788	XANG1	78C
794	XSLMAX	798	ELLIPT	79C	HAFSLP	7A0
7A8	XHAF2	7AC	SLPAT	7B0	PINC	7B4
7BC	XPAGE	7C0	IPEN	7C4	II	7C8
7DC	YPAGE	7D4				

ARRAY MAP

LOCATION	SYMBOL	LOCATION	SYMBOL	LOCATION	SYMBOL	LOCATIO
708	X	4658	IN	5918	OUT	6BD8
9158						

FORMAT STATEMENT MAP

LOCATION	SYMBOL	LOCATION	SYMBOL	LOCATION	SYMBOL	LOCATIO
A45C	200	A45B	220	A473	300	A48B
A4A8	3	A4E0	70	A4F7	998	A54A
A5E5	68	A5EA	69	A640	405	A673

IN EFFECT* ID,EBCDIC,SOURCE,NOLIST,NODECK,LOAD,MAP
IN EFFECT* NAME = MAIN , LINECNT = 60
ICS* SOURCE STATEMENTS = 301,PROGRAM SIZE = 51544
ICS* NO DIAGNOSTICS GENERATED